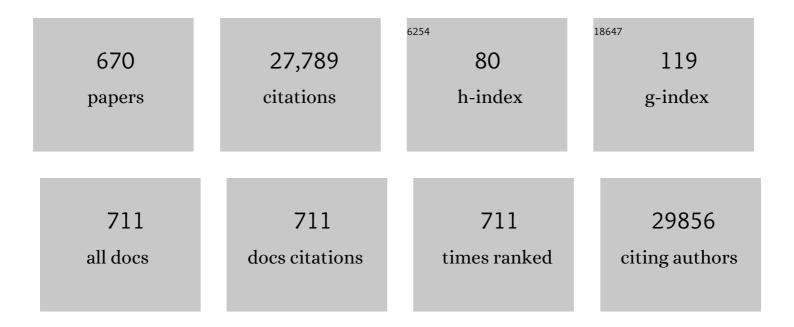
List of Publications by Year in descending order

Source: https://exaly.com/author-pdf/7083221/publications.pdf Version: 2024-02-01



#	Article	IF	CITATIONS
1	Facile and secure synthesis of porous partially fluorinated graphene employing weakly coordinating anion for enhanced high-performance symmetric supercapacitor. Journal of Materiomics, 2022, 8, 113-122.	5.7	8
2	Electrochemical and electronic detection of biomarkers in serum: a systematic comparison using aptamer-functionalized surfaces. Analytical and Bioanalytical Chemistry, 2022, 414, 5319-5327.	3.7	9
3	Surface modification of silicon nanowires for biosensing. , 2022, , 25-68.		1
4	Efficient detoxification of Cr(VI)-containing effluents by sequential adsorption and reduction using a novel cysteine-doped PANi@faujasite composite: Experimental study supported by advanced statistical physics prediction. Journal of Hazardous Materials, 2022, 422, 126857.	12.4	65
5	Biocompatibility of semiconducting silicon nanowires. , 2022, , 69-110.		0
6	Facile Synthesis of Bimetal Nickel Cobalt Phosphate Nanostructures for High-Performance Hybrid Supercapacitors. Journal of Alloys and Compounds, 2022, 893, 162340.	5.5	32
7	Synthesis and characterization of palladium nanoparticles immobilized on graphene oxide functionalized with triethylenetetramine or 2,6-diaminopyridine and application for the Suzuki cross-coupling reaction. Journal of Organometallic Chemistry, 2022, 957, 122160.	1.8	14
8	A green and sensitive guanine-based DNA biosensor for idarubicin anticancer monitoring in biological samples: A simple and fast strategy for control of health quality in chemotherapy procedure confirmed by docking investigation. Chemosphere, 2022, 291, 132928.	8.2	194
9	A newly synthesized bipyridineâ€containing manganese( <scp>II</scp> ) complex immobilized on graphene oxide as active electrocatalyst for hydrogen gas production from alkaline solutions: Experimental and theoretical studies. International Journal of Energy Research, 2022, 46, 6577-6593.	4.5	2
10	Emerging advances and current applications of nanoMOF-based membranes for water treatment. Chemosphere, 2022, 292, 133369.	8.2	13
11	An efficient CuO/rGO/TiO <sub>2</sub> photocatalyst for the synthesis of benzopyranopyrimidine compounds under visible light irradiation. New Journal of Chemistry, 2022, 46, 3817-3830.	2.8	8
12	Photothermal Activatable Mucoadhesive Fiber Mats for On-Demand Delivery of Insulin via Buccal and Corneal Mucosa. ACS Applied Bio Materials, 2022, 5, 771-778.	4.6	14
13	Innovative transdermal delivery of insulin using gelatin methacrylate-based microneedle patches in mice and mini-pigs. Nanoscale Horizons, 2022, 7, 174-184.	8.0	21
14	The holy grail of pyrene-based surface ligands on the sensitivity of graphene-based field effect transistors. Sensors & Diagnostics, 2022, 1, 235-244.	3.8	17
15	Effectiveness of a novel polyaniline@Fe-ZSM-5 hybrid composite for Orange G dye removal from aqueous media: Experimental study and advanced statistical physics insights. Chemosphere, 2022, 295, 133786.	8.2	39
16	Impact of colistin and colistin-loaded on alginate nanoparticles on pigs infected with a colistin-resistant enterotoxigenic Escherichia coli strain. Veterinary Microbiology, 2022, 266, 109359.	1.9	3
17	Highly performing graphene-based field effect transistor for the differentiation between mild-moderate-severe myocardial injury. Nano Today, 2022, 43, 101391.	11.9	24
18	Colorimetric assay for the detection of dopamine using bismuth ferrite oxide (Bi2Fe4O9) nanoparticles as an efficient peroxidase-mimic nanozyme. Journal of Colloid and Interface Science, 2022, 613, 384-395.	9.4	33

#	Article	IF	CITATIONS
19	Synthesis and characterization of a novel multi-functionalized reduced graphene oxide as a pH-sensitive drug delivery material and a photothermal candidate. Applied Surface Science, 2022, 583, 152568.	6.1	14
20	Phytic acid-doped poly- <i>N</i> -phenylglycine potato peels for removal of anionic dyes: investigation of adsorption parameters. New Journal of Chemistry, 2022, 46, 5111-5120.	2.8	3
21	Surface modification of carbon dots with tetraalkylammonium moieties for fine tuning their antibacterial activity. Materials Science and Engineering C, 2022, 134, 112697.	7.3	10
22	Electrocatalytic hydrogen generation using tripod containing pyrazolylborate-based copper( <scp>ii</scp> ), nickel( <scp>ii</scp> ), and iron( <scp>iii</scp> ) complexes loaded on a glassy carbon electrode. RSC Advances, 2022, 12, 8030-8042.	3.6	3
23	Effective PDT/PTT dual-modal phototherapeutic killing of bacteria by using poly(N-phenylglycine) nanoparticles. Mikrochimica Acta, 2022, 189, 150.	5.0	3
24	Adsorption-reduction of Cr(VI) onto unmodified and phytic acid-modified carob waste: Kinetic and isotherm modeling. Chemosphere, 2022, 297, 134188.	8.2	14
25	Catch and release strategy of matrix metalloprotease aptamers <i>via</i> thiol–disulfide exchange reaction on a graphene based electrochemical sensor. Sensors & Diagnostics, 2022, 1, 739-749.	3.8	4
26	Cathodic Activation of Titania-Fly Ash Cenospheres for Efficient Electrochemical Hydrogen Production: A Proposed Solution to Treat Fly Ash Waste. Catalysts, 2022, 12, 466.	3.5	2
27	Preparation of nanowires on free-standing boron-doped diamond films for high performance micro-capacitors. Electrochimica Acta, 2022, 421, 140500.	5.2	3
28	Single‣tep Synthesis of Exfoliated Ti <sub>3</sub> C <sub>2</sub> T <sub>x</sub> MXene through NaBF <sub>4</sub> /HCl Etching as Electrode Material for Asymmetric Supercapacitor. ChemistrySelect, 2022, 7, .	1.5	6
29	Electrochemical H2 Production using Polypyrazole based Zinc(II) Complex in Alkaline Medium. Asian Journal of Chemistry, 2022, 34, 1366-1372.	0.3	0
30	Enhancing Colistin Activity against Colistin-Resistant Escherichia coli through Combination with Alginate Nanoparticles and Small Molecules. Pharmaceuticals, 2022, 15, 682.	3.8	2
31	Influence of graphene oxide on the toxicity of polystyrene nanoplastics to the marine microalgae Picochlorum sp Environmental Science and Pollution Research, 2022, 29, 75870-75882.	5.3	2
32	Enhanced Antibacterial Activity of Dermaseptin through Its Immobilization on Alginate Nanoparticles—Effects of Menthol and Lactic Acid on Its Potentialization. Antibiotics, 2022, 11, 787.	3.7	2
33	TRPM8 as an Anti–Tumoral Target in Prostate Cancer Growth and Metastasis Dissemination. International Journal of Molecular Sciences, 2022, 23, 6672.	4.1	9
34	Magnetic MnFe2O4 Core–shell nanoparticles coated with antibiotics for the ablation of pathogens. Chemical Papers, 2021, 75, 377-387.	2.2	10
35	Colorimetric sensing of dopamine in beef meat using copper sulfide encapsulated within bovine serum albumin functionalized with copper phosphate (CuS-BSA-Cu3(PO4)2) nanoparticles. Journal of Colloid and Interface Science, 2021, 582, 732-740.	9.4	35
36	Facile synthesis and characterization of a novel 1,2,4,5-benzene tetracarboxylic acid doped polyaniline@zinc phosphate nanocomposite for highly efficient removal of hazardous hexavalent chromium ions from water. Journal of Colloid and Interface Science, 2021, 585, 560-573.	9.4	87

#	Article	IF	CITATIONS
37	The impact of chemical engineering and technological advances on managing diabetes: present and future concepts. Chemical Society Reviews, 2021, 50, 2102-2146.	38.1	28
38	Simultaneous photocatalytic Cr(VI) reduction and phenol degradation over copper sulphide-reduced graphene oxide nanocomposite under visible light irradiation: Performance and reaction mechanism. Chemosphere, 2021, 268, 128798.	8.2	47
39	Reduced graphene oxide–based field effect transistors for the detection of E7 protein of human papillomavirus in saliva. Analytical and Bioanalytical Chemistry, 2021, 413, 779-787.	3.7	62
40	SERS characterization of aggregated and isolated bacteria deposited on silver-based substrates. Analytical and Bioanalytical Chemistry, 2021, 413, 1417-1428.	3.7	18
41	CoS <sub>2</sub> Nanoparticles Supported on rGO, g-C <sub>3</sub> N <sub>4</sub> , BCN, MoS <sub>2</sub> , and WS <sub>2</sub> Two-Dimensional Nanosheets with Excellent Electrocatalytic Performance for Overall Water Splitting: Electrochemical Studies and DFT Calculations. ACS Applied Energy Materials. 2021. 4. 1269-1285.	5.1	39
42	Carbon quantum dots as a dual platform for the inhibition and light-based destruction of collagen fibers: implications for the treatment of eye floaters. Nanoscale Horizons, 2021, 6, 449-461.	8.0	14
43	Aryne cycloaddition reaction as a facile and mild modification method for design of electrode materials for high-performance symmetric supercapacitor. Electrochimica Acta, 2021, 369, 137667.	5.2	8
44	The Potential of Developing Pan-Coronaviral Antibodies to Spike Peptides in Convalescent COVID-19 Patients. Archivum Immunologiae Et Therapiae Experimentalis, 2021, 69, 5.	2.3	8
45	<i>In Situ</i> Synthesis of Co <sub>3</sub> O <sub>4</sub> /CoFe <sub>2</sub> O <sub>4</sub> Derived from a Metal–Organic Framework on Nickel Foam: High-Performance Electrocatalyst for Water Oxidation. ACS Applied Energy Materials, 2021, 4, 2951-2959.	5.1	34
46	Cathodic pre-polarization studies on the carbon felt/KOH interface: An efficient metal-free electrocatalyst for hydrogen generation. Electrochimica Acta, 2021, 375, 137981.	5.2	8
47	Modification of MnFe2O4 surface by Mo (VI) pyridylimine complex as an efficient nanocatalyst for (ep)oxidation of alkenes and sulfides. Journal of Molecular Liquids, 2021, 330, 115690.	4.9	16
48	Colorimetric detection of chromium (VI) ion using poly(N-phenylglycine) nanoparticles acting as a peroxidase mimetic catalyst. Talanta, 2021, 226, 122082.	5.5	32
49	Morphological influence of BiVO4 nanostructures on peroxymonosulfate activation for highly efficient catalytic degradation of rhodamine B. Environmental Science and Pollution Research, 2021, 28, 52236-52246.	5.3	12
50	Enhanced electrocatalytic activity of PtRu/nitrogen and sulphur co-doped crumbled graphene in acid and alkaline media. Journal of Colloid and Interface Science, 2021, 590, 154-163.	9.4	13
51	Efficacious Alkaline Copper Corrosion Inhibition by a Mixed Ligand Copper(II) Complex of 2,2′â€Bipyridine and Glycine: Electrochemical and Theoretical Studies. ChemElectroChem, 2021, 8, 2052-2064.	3.4	7
52	Carbon–nitrogen bond formation using modified graphene oxide derivatives decorated with copper complexes and nanoparticles. Applied Organometallic Chemistry, 2021, 35, e6327.	3.5	5
53	Natural antibodies: Protecting role of IgM in glioblastoma and brain tumours. Current Pharmaceutical Design, 2021, 27, 4515-4529.	1.9	Ο
54	Rapid Generation of Coronaviral Immunity Using Recombinant Peptide Modified Nanodiamonds. Pathogens, 2021, 10, 861.	2.8	10

#	Article	IF	CITATIONS
55	Au-assisted Polymerization of Conductive Poly(N-phenylglycine) as High-performance Positive Electrodes for Asymmetric Supercapacitors. Nanotechnology, 2021, 33, .	2.6	1
56	Flowerâ€like Nitrogenâ€coâ€doped MoS <sub>2</sub> @RGO Composites with Excellent Stability for Supercapacitors. ChemElectroChem, 2021, 8, 2903-2911.	3.4	12
57	Graphene-Induced Hyperthermia (GIHT) Combined With Radiotherapy Fosters Immunogenic Cell Death. Frontiers in Oncology, 2021, 11, 664615.	2.8	13
58	Enhanced Antibacterial Activity of CuS-BSA/Lysozyme under Near Infrared Light Irradiation. Nanomaterials, 2021, 11, 2156.	4.1	11
59	Enhanced visible light-triggered antibacterial activity of carbon quantum dots/polyurethane nanocomposites by gamma rays induced pre-treatment. Radiation Physics and Chemistry, 2021, 185, 109499.	2.8	15
60	The importance of the shape of Cu2O nanocrystals on plasmon-enhanced oxygen evolution reaction in alkaline media. Electrochimica Acta, 2021, 390, 138810.	5.2	11
61	Development of a novel PANI@WO3 hybrid composite and its application as a promising adsorbent for Cr(VI) ions removal. Journal of Environmental Chemical Engineering, 2021, 9, 105885.	6.7	55
62	Cobalt sulfide-reduced graphene oxide: An efficient catalyst for the degradation of rhodamine B and pentachlorophenol using peroxymonosulfate. Journal of Environmental Chemical Engineering, 2021, 9, 106018.	6.7	20
63	Magnetically driven superhydrophobic/superoleophilic graphene-based polyurethane sponge for highly efficient oil/water separation and demulsification. Separation and Purification Technology, 2021, 274, 118931.	7.9	80
64	A mask-based diagnostic platform for point-of-care screening of Covid-19. Biosensors and Bioelectronics, 2021, 192, 113486.	10.1	29
65	Silicon nanowire-hydrogenated TiO2 core-shell arrays for stable electrochemical micro-capacitors. Electrochimica Acta, 2021, 396, 139198.	5.2	6
66	Self-combustion synthesis of dilithium cobalt bis(tungstate) decorated with silver nanoparticles for high performance hybrid supercapacitors. Chemical Engineering Journal, 2021, 426, 131252.	12.7	16
67	Ultra-sensitive and fast optical detection of the spike protein of the SARS-CoV-2 using AgNPs/SiNWs nanohybrid based sensors. Surfaces and Interfaces, 2021, 27, 101454.	3.0	27
68	Alginate Nanoparticles Enhance Anti-Clostridium perfringens Activity of the Leaderless Two-Peptide Enterocin DD14 and Affect Expression of Some Virulence Factors. Probiotics and Antimicrobial Proteins, 2021, 13, 1213-1227.	3.9	10
69	Controlled covalent functionalization of a graphene-channel of a field effect transistor as an ideal platform for (bio)sensing applications. Nanoscale Horizons, 2021, 6, 819-829.	8.0	24
70	Diaryl Sulfide Derivatives as Potential Iron Corrosion Inhibitors: A Computational Study. Molecules, 2021, 26, 6312.	3.8	3
71	Fabrication of superhydrophobic/superoleophilic functionalized reduced graphene oxide/polydopamine/PFDT membrane for efficient oil/water separation. Separation and Purification Technology, 2020, 236, 116240.	7.9	42
72	Preparation of magnetic, superhydrophobic/superoleophilic polyurethane sponge: Separation of oil/water mixture and demulsification. Chemical Engineering Journal, 2020, 384, 123339.	12.7	144

#	Article	IF	CITATIONS
73	High performance of 3D silicon nanowires array@CrN for electrochemical capacitors. Nanotechnology, 2020, 31, 035407.	2.6	8
74	Electrothermal patches driving the transdermal delivery of insulin. Nanoscale Horizons, 2020, 5, 663-670.	8.0	30
75	Highly efficient conversion of the nitroarenes to amines at the interface of a ternary hybrid containing silver nanoparticles doped reduced graphene oxide/ graphitic carbon nitride under visible light. Journal of Hazardous Materials, 2020, 387, 121700.	12.4	36
76	Functionalized MoS2/polyurethane sponge: An efficient scavenger for oil in water. Separation and Purification Technology, 2020, 238, 116420.	7.9	37
77	Mussel-Inspired Superhydrophobic Surfaces on 316L Stainless Steel with Enhanced Corrosion Resistance. Metallurgical and Materials Transactions A: Physical Metallurgy and Materials Science, 2020, 51, 909-919.	2.2	9
78	MnOx thin film based electrodes: Role of surface point defects and structure towards extreme enhancement in specific capacitance. Materials Chemistry and Physics, 2020, 242, 122487.	4.0	10
79	Design and preparation of core-shell structured magnetic graphene oxide@MIL-101(Fe): Photocatalysis under shell to remove diazinon and atrazine pesticides. Solar Energy, 2020, 208, 990-1000.	6.1	41
80	Electrochemical, theoretical and surface physicochemical studies of the alkaline copper corrosion inhibition by newly synthesized molecular complexes of benzenediamine and tetraamine with π acceptor. Journal of Molecular Liquids, 2020, 320, 114386.	4.9	8
81	Cu <sub>2</sub> 0/reduced graphene oxide/TiO <sub>2</sub> nanomaterial: An effective photocatalyst for azideâ€elkyne cycloaddition with benzyl halides or epoxide derivatives under visible light irradiation. Applied Organometallic Chemistry, 2020, 34, e5928.	3.5	19
82	Preparation of boron-doped diamond nanospikes on porous Ti substrate for high-performance supercapacitors. Electrochimica Acta, 2020, 354, 136649.	5.2	14
83	Magnetic polyurethane sponge for efficient oil adsorption and separation of oil from oil-in-water emulsions. Separation and Purification Technology, 2020, 240, 116627.	7.9	93
84	Synthesis and characterization of arginine-doped polyaniline/walnut shell hybrid composite with superior clean-up ability for chromium (VI) from aqueous media: Equilibrium, reusability and process optimization. Journal of Molecular Liquids, 2020, 316, 113832.	4.9	84
85	New Bacteriocins from Lacticaseibacillus paracasei CNCM I-5369 Adsorbed on Alginate Nanoparticles Are Very Active against Escherichia coli. International Journal of Molecular Sciences, 2020, 21, 8654.	4.1	11
86	Plasmon-Driven Electrochemical Methanol Oxidation on Gold Nanohole Electrodes. ACS Applied Materials & Interfaces, 2020, 12, 50426-50432.	8.0	21
87	Cathodic activation of synthesized highly defective monoclinic hydroxylâ€functionalized <scp> ZrO <sub>2</sub> </scp> nanoparticles for efficient electrochemical production of hydrogen in alkaline media. International Journal of Energy Research, 2020, 44, 10695-10709.	4.5	9
88	Cellulose Nanocrystals/Graphene Hybrids—A Promising New Class of Materials for Advanced Applications. Nanomaterials, 2020, 10, 1523.	4.1	109
89	An â€~on-demand' photothermal antibiotic release cryogel patch: evaluation of efficacy on an <i>ex vivo</i> model for skin wound infection. Biomaterials Science, 2020, 8, 5911-5919.	5.4	27
90	Formation of a Highly Stable and Nontoxic Protein Corona upon Interaction of Human α-1-Acid Glycoprotein (AGP) with Citrate-Stabilized Silver Nanoparticles. Langmuir, 2020, 36, 10321-10330.	3.5	18

#	Article	IF	CITATIONS
91	Photothermally Active Cryogel Devices for Effective Release of Antimicrobial Peptides: On-Demand Treatment of Infections. ACS Applied Materials & Interfaces, 2020, 12, 56805-56814.	8.0	22
92	Nanodiamonds for bioapplications, recent developments. Journal of Materials Chemistry B, 2020, 8, 10878-10896.	5.8	33
93	Plasmon-enhanced electrocatalytic oxygen reduction in alkaline media on gold nanohole electrodes. Journal of Materials Chemistry A, 2020, 8, 10395-10401.	10.3	12
94	Pt–ZnO/M (M = Fe, Co, Ni or Cu): A New Promising Hybrid-Doped Noble Metal/Semiconductor Photocatalysts. Journal of Inorganic and Organometallic Polymers and Materials, 2020, 30, 4627-4636.	3.7	7
95	Rapid and sensitive identification of uropathogenic Escherichia coli using a surface-enhanced-Raman-scattering-based biochip. Talanta, 2020, 219, 121174.	5.5	16
96	The antimicrobial peptide oranicin P16 isolated from Trichosporon asahii ICVY021, found in camel milk's, inhibits Kocuria rhizophila. Food Bioscience, 2020, 36, 100670.	4.4	6
97	NiMnCr layered double hydroxide-carbon spheres modified Ni foam: An efficient positive electrode for hybrid supercapacitors. Chemical Engineering Journal, 2020, 396, 125370.	12.7	27
98	Graphene oxide chemically reduced and functionalized with KOH-PEI for efficient Cr(VI) adsorption and reduction in acidic medium. Chemosphere, 2020, 258, 127316.	8.2	77
99	Heterologous Biosynthesis of Five New Class II Bacteriocins From Lactobacillus paracasei CNCM I-5369 With Antagonistic Activity Against Pathogenic Escherichia coli Strains. Frontiers in Microbiology, 2020, 11, 1198.	3.5	21
100	Aluminum based metal-organic framework integrated with reduced graphene oxide for improved supercapacitive performance. Electrochimica Acta, 2020, 353, 136609.	5.2	21
101	Plasmon-induced photocatalytic transformations. , 2020, , 249-275.		0
102	Graphene Oxide Nanosheets for Localized Hyperthermia—Physicochemical Characterization, Biocompatibility, and Induction of Tumor Cell Death. Cells, 2020, 9, 776.	4.1	16
103	Nanoscale materials for the treatment of water contaminated by bacteria and viruses. , 2020, , 261-305.		3
104	High performance of phytic acid-functionalized spherical poly-phenylglycine particles for removal of heavy metal ions. Applied Surface Science, 2020, 518, 146206.	6.1	28
105	High performance flexible hybrid supercapacitors based on nickel hydroxide deposited on copper oxide supported by copper foam for a sunlight-powered rechargeable energy storage system. Journal of Colloid and Interface Science, 2020, 579, 520-530.	9.4	33
106	Magneto-Optical Nanostructures for Viral Sensing. Nanomaterials, 2020, 10, 1271.	4.1	13
107	High-performance flexible hybrid supercapacitor based on NiAl layered double hydroxide as a positive electrode and nitrogen-doped reduced graphene oxide as a negative electrode. Electrochimica Acta, 2020, 354, 136664.	5.2	19
108	Copperâ€based metal–organic framework decorated by CuO hairâ€like nanostructures: Electrocatalyst for oxygen evolution reaction. Applied Organometallic Chemistry, 2020, 34, e5871.	3.5	11

#	Article	IF	CITATIONS
109	Surface Functionalization with Polyethylene Glycol and Polyethyleneimine Improves the Performance of Graphene-Based Materials for Safe and Efficient Intracellular Delivery by Laser-Induced Photoporation. International Journal of Molecular Sciences, 2020, 21, 1540.	4.1	17
110	Ultrasmall CuS-BSA-Cu3(PO4)2 nanozyme for highly efficient colorimetric sensing of H2O2 and glucose in contact lens care solutions and human serum. Analytica Chimica Acta, 2020, 1109, 78-89.	5.4	34
111	Pd nanoparticles supported on reduced graphene oxide as an effective and reusable heterogeneous catalyst for the Mizoroki–Heck coupling reaction. Applied Organometallic Chemistry, 2020, 34, e5524.	3.5	29
112	Long-term live-cell microscopy with labeled nanobodies delivered by laser-induced photoporation. Nano Research, 2020, 13, 485-495.	10.4	14
113	Enhanced electrocatalytic hydrogen evolution on a plasmonic electrode: the importance of the Ti/TiO2 adhesion layer. Journal of Materials Chemistry A, 2020, 8, 13980-13986.	10.3	10
114	Interaction of cellulose and nitrodopamine coated superparamagnetic iron oxide nanoparticles with alpha-lactalbumin. RSC Advances, 2020, 10, 9704-9716.	3.6	14
115	Flexible Energy Storage Device Based on Poly( <i>N</i> -phenylglycine), an Incentive-Energy Pseudocapacitive Conducting Polymer, and Electrochemically Exfoliated Graphite Sheets. ACS Sustainable Chemistry and Engineering, 2020, 8, 6433-6441.	6.7	20
116	Crystalline <scp>ZnO</scp> and <scp>ZnO</scp> / <scp> TiO <sub>2</sub> </scp> nanoparticles derived from <i>tert</i> â€butyl Nâ€{2 mercaptoethyl)carbamatozinc( <scp>II</scp> ) chelate: Electrocatalytic studies for <scp> H <sub>2</sub> </scp> generation in alkaline electrolytes. International Journal of Energy Research, 2020, 44, 6725-6744.	4.5	11
117	Ultrasound Assisted the Synthesis of 1,3-Dioxolane Derivatives from the Reaction of Epoxides or 1,2-Diols with Various Ketones Using Graphene Oxide Catalyst. Catalysis Letters, 2020, 150, 2959-2969.	2.6	9
118	Purification for Carbon Nanotubes Synthesized by Flame Fragments Deposition via Hydrogen Peroxide and Acetone. Materials, 2020, 13, 2342.	2.9	21
119	Efficient and Regioselective Ring-opening of Epoxides with Carboxylic Acid Catalyzed by Graphite Oxide. Letters in Organic Chemistry, 2020, 17, 532-538.	0.5	2
120	Fast and facile preparation of nanostructured silicon surfaces for laser desorption/ionization mass spectrometry of small compounds. Rapid Communications in Mass Spectrometry, 2019, 33, 66-74.	1.5	8
121	CoO Promoted the Catalytic Activity of Nitrogen-Doped MoS <sub>2</sub> Supported on Carbon Fibers for Overall Water Splitting. ACS Applied Materials & Interfaces, 2019, 11, 31889-31898.	8.0	72
122	Robust superhydrophobic polyurethane sponge functionalized with perfluorinated graphene oxide for efficient immiscible oil/water mixture, stable emulsion separation and crude oil dehydration. Science China Technological Sciences, 2019, 62, 1585-1595.	4.0	28
123	Ag and Au nanoparticles/reduced graphene oxide composite materials: Synthesis and application in diagnostics and therapeutics. Advances in Colloid and Interface Science, 2019, 271, 101991.	14.7	102
124	Chitosan/hydroxyapatite modified carbon/carbon composites: synthesis, characterization and <i>in vitro</i> biocompatibility evaluation. RSC Advances, 2019, 9, 23362-23372.	3.6	11
125	Toxicity Effect of Silver Nanoparticles on Photosynthetic Pigment Content, Growth, ROS Production and Ultrastructural Changes of Microalgae Chlorella vulgaris. Nanomaterials, 2019, 9, 914.	4.1	48
126	Dopamine-functionalized cyclodextrins: modification of reduced graphene oxide based electrodes and sensing of folic acid in human serum. Analytical and Bioanalytical Chemistry, 2019, 411, 5149-5157.	3.7	10

#	Article	IF	CITATIONS
127	662 Bacterial infection and wound healing in an ex vivo human skin model. Journal of Investigative Dermatology, 2019, 139, S328.	0.7	1
128	Functional Carbon Quantum Dots as Medical Countermeasures to Human Coronavirus. ACS Applied Materials & Interfaces, 2019, 11, 42964-42974.	8.0	231
129	Self-template synthesis of ZnS/Ni3S2 as advanced electrode material for hybrid supercapacitors. Electrochimica Acta, 2019, 328, 135065.	5.2	32
130	High spatial resolution electrochemical biosensing using reflected light microscopy. Scientific Reports, 2019, 9, 15196.	3.3	10
131	Preparation of Low-Resistance and Residue-free ITO Films for Large-scale 3D Displays. ACS Applied Materials & Interfaces, 2019, 11, 45903-45913.	8.0	9
132	CuS Decorated Functionalized Reduced Graphene Oxide: A Dual Responsive Nanozyme for Selective Detection and Photoreduction of Cr(VI) in an Aqueous Medium. ACS Sustainable Chemistry and Engineering, 2019, 7, 16131-16143.	6.7	63
133	Achieving on chip micro-supercapacitors based on CrN deposited by bipolar magnetron sputtering at glancing angle. Electrochimica Acta, 2019, 324, 134890.	5.2	35
134	LB1138 An ex vivo human skin model for healing of infected wounds. Journal of Investigative Dermatology, 2019, 139, B24.	0.7	1
135	Mucin modified SPR interfaces for studying the effect of flow on pathogen binding to Atlantic salmon mucins. Biosensors and Bioelectronics, 2019, 146, 111736.	10.1	10
136	Cu(0) nanoparticle-decorated functionalized reduced graphene oxide sheets as artificial peroxidase enzymes: application for colorimetric detection of Cr( <scp>vi</scp> ) ions. New Journal of Chemistry, 2019, 43, 1404-1414.	2.8	23
137	Plasmon-Induced Electrocatalysis with Multi-Component Nanostructures. Materials, 2019, 12, 43.	2.9	17
138	Heterostructures of mesoporous TiO2 and SnO2 nanocatalyst for improved electrochemical oxidation ability of vitamin B6 in pharmaceutical tablets. Journal of Colloid and Interface Science, 2019, 542, 45-53.	9.4	35
139	Efficient oil/water separation by superhydrophobic CuxS coated on copper mesh. Separation and Purification Technology, 2019, 215, 573-581.	7.9	64
140	Phenyl-grafted carbon nitride semiconductor for photocatalytic CO <sub>2</sub> -reduction and rapid degradation of organic dyes. Catalysis Science and Technology, 2019, 9, 822-832.	4.1	39
141	Graphene oxide effects in early ontogenetic stages of Triticum aestivum L. seedlings. Ecotoxicology and Environmental Safety, 2019, 181, 345-352.	6.0	39
142	Excellent photocatalytic reduction of nitroarenes to aminoarenes by BiVO <sub>4</sub> nanoparticles grafted on reduced graphene oxide (rGO/BiVO <sub>4</sub> ). Applied Organometallic Chemistry, 2019, 33, e5059.	3.5	19
143	Carbon-based quantum particles: an electroanalytical and biomedical perspective. Chemical Society Reviews, 2019, 48, 4281-4316.	38.1	187
144	Phytic acid-doped polyaniline nanofibers-clay mineral for efficient adsorption of copper (II) ions. Journal of Colloid and Interface Science, 2019, 553, 688-698.	9.4	57

#	Article	IF	CITATIONS
145	Manganese Ferrite Nanoparticles Modified by Mo(VI) Complex: Highly Efficient Catalyst for Sulfides and Olefins Oxidation Under Solventâ€less Condition. ChemistrySelect, 2019, 4, 7116-7122.	1.5	6
146	Near-infrared light activatable hydrogels for metformin delivery. Nanoscale, 2019, 11, 15810-15820.	5.6	30
147	Fabrication of ZnCoS nanomaterial for high energy flexible asymmetric supercapacitors. Chemical Engineering Journal, 2019, 374, 347-358.	12.7	72
148	Dual-Ligand Fe-Metal Organic Framework Based Robust High Capacity Li Ion Battery Anode and Its Use in a Flexible Battery Format for Electro-Thermal Heating. ACS Applied Energy Materials, 2019, 2, 4450-4457.	5.1	35
149	Encapsulation of a TRPM8 Agonist, WS12, in Lipid Nanocapsules Potentiates PC3 Prostate Cancer Cell Migration Inhibition through Channel Activation. Scientific Reports, 2019, 9, 7926.	3.3	22
150	A facile preparation of CuS-BSA nanocomposite as enzyme mimics: Application for selective and sensitive sensing of Cr(VI) ions. Sensors and Actuators B: Chemical, 2019, 294, 253-262.	7.8	64
151	Exploring Light-Sensitive Nanocarriers for Simultaneous Triggered Antibiotic Release and Disruption of Biofilms Upon Generation of Laser-Induced Vapor Nanobubbles. Pharmaceutics, 2019, 11, 201.	4.5	26
152	High performance silicon nanowires/ruthenium nanoparticles micro-supercapacitors. Electrochimica Acta, 2019, 311, 150-159.	5.2	30
153	The Influence of Microstructure on the Passive Layer Chemistry and Corrosion Resistance for Some Titanium-Based Alloys. Materials, 2019, 12, 1233.	2.9	17
154	High-Energy Flexible Supercapacitor—Synergistic Effects of Polyhydroquinone and RuO <sub>2</sub> · <i>x</i> H <sub>2</sub> O with Microsized, Few-Layered, Self-Supportive Exfoliated-Graphite Sheets. ACS Applied Materials & Interfaces, 2019, 11, 18349-18360.	8.0	49
155	Synthesis and photocatalytic efficiency of sol-gel Al3+-doped TiO2 thin films: correlation between the structural, morphological and optical properties. Materials Research Express, 2019, 6, 085036.	1.6	2
156	One-pot green synthesis of reduced graphene oxide decorated with β-Ni(OH)2-nanoflakes as an efficient electrochemical platform for the determination of antipsychotic drug sulpiride. Microchemical Journal, 2019, 147, 555-563.	4.5	14
157	"Click―Chemistry on Gold Electrodes Modified with Reduced Graphene Oxide by Electrophoretic Deposition. Surfaces, 2019, 2, 193-204.	2.3	15
158	ZnO/Carbon nanowalls shell/core nanostructures as electrodes for supercapacitors. Applied Surface Science, 2019, 481, 926-932.	6.1	35
159	Efficient capture and photothermal ablation of planktonic bacteria and biofilms using reduced graphene oxide–polyethyleneimine flexible nanoheaters. Journal of Materials Chemistry B, 2019, 7, 2771-2781.	5.8	31
160	Interaction of Human α-1-Acid Glycoprotein (AGP) with Citrate-Stabilized Gold Nanoparticles: Formation of Unexpectedly Strong Binding Events. Journal of Physical Chemistry C, 2019, 123, 5073-5083.	3.1	10
161	Electrochemical cardiovascular platforms: Current state of the art and beyond. Biosensors and Bioelectronics, 2019, 131, 287-298.	10.1	55
162	Graphene-modified electrodes for sensing doxorubicin hydrochloride in human plasma. Analytical and Bioanalytical Chemistry, 2019, 411, 1509-1516.	3.7	39

#	Article	IF	CITATIONS
163	Palladium oxide nanoparticles supported on graphene oxide: A convenient heterogeneous catalyst for reduction of various carbonyl compounds using triethylsilane. Applied Organometallic Chemistry, 2019, 33, e4837.	3.5	19
164	Highly improved photoreduction of carbon dioxide to methanol using cobalt phthalocyanine grafted to graphitic carbon nitride as photocatalyst under visible light irradiation. Journal of Colloid and Interface Science, 2019, 543, 201-213.	9.4	70
165	Aluminum oxide nanowires as safe and effective adjuvants for next-generation vaccines. Materials Today, 2019, 22, 58-66.	14.2	30
166	PMS activation using reduced graphene oxide under sonication: Efficient metal-free catalytic system for the degradation of rhodamine B, bisphenol A, and tetracycline. Ultrasonics Sonochemistry, 2019, 52, 164-175.	8.2	89
167	Preparation of superhydrophobic/superoleophilic copper coated titanium mesh with excellent ice-phobic and water-oil separation performance. Applied Surface Science, 2019, 476, 353-362.	6.1	30
168	Core-shell Ni/NiO grafted cobalt (II) complex: An efficient inorganic nanocomposite for photocatalytic reduction of CO2 under visible light irradiation. Applied Surface Science, 2019, 467-468, 370-381.	6.1	49
169	Evaporation behavior of PEGylated graphene oxide nanofluid droplets on heated substrate. International Journal of Thermal Sciences, 2019, 135, 445-458.	4.9	23
170	Entrapment of uropathogenic E. coli cells into ultra-thin sol-gel matrices on gold thin films: A low cost alternative for impedimetric bacteria sensing. Biosensors and Bioelectronics, 2019, 124-125, 161-166.	10.1	29
171	Graphite/Nanocrystalline Zeolite Platform for Selective Electrochemical Determination of Hepatitis C Inhibitor Ledipasvir. Electroanalysis, 2019, 31, 1215-1223.	2.9	12
172	Efficient reduction of Cr(VI) under visible light irradiation using CuS nanostructures. Arabian Journal of Chemistry, 2019, 12, 215-224.	4.9	40
173	Extraction of Cellulose Nanocrystals with Structure I and II and Their Applications for Reduction of Graphene Oxide and Nanocomposite Elaboration. Waste and Biomass Valorization, 2019, 10, 1913-1927.	3.4	35
174	NiFe layered double hydroxide electrodeposited on Ni foam coated with reduced graphene oxide for high-performance supercapacitors. Electrochimica Acta, 2019, 302, 1-9.	5.2	89
175	Interaction of 4 allotropic modifications of carbon nanoparticles with living tissues. Ukrainian Biochemical Journal, 2019, 91, 41-50.	0.5	4
176	Facile preparation of high density polyethylene superhydrophobic/superoleophilic coatings on glass, copper and polyurethane sponge for self-cleaning, corrosion resistance and efficient oil/water separation. Journal of Colloid and Interface Science, 2018, 525, 76-85.	9.4	55
177	Graphene-based biosensors. Interface Focus, 2018, 8, 20160132.	3.0	110
178	Aqueous medium-induced micropore formation in plasma polymerized polystyrene: an effective route to inhibit bacteria adhesion. Journal of Materials Chemistry B, 2018, 6, 3674-3683.	5.8	1
179	Effect of high Fe doping on Raman modes and optical properties of hydrothermally prepared SnO 2 nanoparticles. Materials Science in Semiconductor Processing, 2018, 77, 31-39.	4.0	44
180	Sensitive electrochemical detection of cardiac troponin I in serum and saliva by nitrogen-doped porous reduced graphene oxide electrode. Sensors and Actuators B: Chemical, 2018, 262, 180-187.	7.8	108

#	Article	IF	CITATIONS
181	Visible light assisted oxidative coupling of benzylamines using heterostructured nanocomposite photocatalyst. Journal of Photochemistry and Photobiology A: Chemistry, 2018, 356, 457-463.	3.9	15
182	Porous reduced graphene oxide modified electrodes for the analysis of protein aggregation. Part 2: Application to the analysis of calcitonin containing pharmaceutical formulation. Electrochimica Acta, 2018, 266, 364-372.	5.2	5
183	Nucleic aptamer modified porous reduced graphene oxide/MoS2 based electrodes for viral detection: Application to human papillomavirus (HPV). Sensors and Actuators B: Chemical, 2018, 262, 991-1000.	7.8	82
184	Reduced graphene oxide/polyethylenimine based immunosensor for the selective and sensitive electrochemical detection of uropathogenic Escherichia coli. Sensors and Actuators B: Chemical, 2018, 260, 255-263.	7.8	86
185	Hydrogen adsorption properties of Ag decorated TiO2 nanomaterials. International Journal of Hydrogen Energy, 2018, 43, 2861-2868.	7.1	35
186	Graphene-based nanomaterials in innovative electrochemistry. Current Opinion in Electrochemistry, 2018, 10, 24-30.	4.8	22
187	Towards green synthesis of monodisperse Cu nanoparticles: An efficient and high sensitive electrochemical nitrite sensor. Sensors and Actuators B: Chemical, 2018, 266, 873-882.	7.8	133
188	Graphene-based bioelectrochemistry and bioelectronics: A concept for the future?. Current Opinion in Electrochemistry, 2018, 12, 141-147.	4.8	7
189	Magnetically Reusable MnFe <sub>2</sub> O <sub>4</sub> Nanoparticles Modified with Oxoâ€Peroxo Mo (VI) Schiffâ€Base Complexes: A High Efficiency Catalyst for Olefin Epoxidation under Solventâ€Free Conditions. ChemistrySelect, 2018, 3, 2877-2881.	1.5	15
190	Controlled modification of electrochemical microsystems with polyethylenimine/reduced graphene oxide using electrophoretic deposition: Sensing of dopamine levels in meat samples. Talanta, 2018, 178, 432-440.	5.5	30
191	Magnetic Fe3O4@V2O5/rGO nanocomposite as a recyclable photocatalyst for dye molecules degradation under direct sunlight irradiation. Chemosphere, 2018, 191, 503-513.	8.2	70
192	One-step immersion for fabrication of superhydrophobic/superoleophilic carbon felts with fire resistance: Fast separation and removal of oil from water. Chemical Engineering Journal, 2018, 331, 372-382.	12.7	48
193	Gold nanoparticles coated silicon nanowires for efficient catalytic and photocatalytic applications. Materials Science in Semiconductor Processing, 2018, 75, 206-213.	4.0	36
194	Cobalt phthalocyanine-supported reduced graphene oxide: A highly efficient catalyst for heterogeneous activation of peroxymonosulfate for rhodamine B and pentachlorophenol degradation. Chemical Engineering Journal, 2018, 336, 465-475.	12.7	72
195	Au Ni alloy nanoparticles supported on reduced graphene oxide as highly efficient electrocatalysts for hydrogen evolution and oxygen reduction reactions. International Journal of Hydrogen Energy, 2018, 43, 1424-1438.	7.1	42
196	Structural and optical characterization of p-type highly Fe-doped SnO2 thin films and tunneling transport on SnO2:Fe/p-Si heterojunction. Applied Surface Science, 2018, 434, 879-890.	6.1	46
197	Near-Infrared Photothermal Heating With Gold Nanostructures. , 2018, , 500-510.		2
198	Electrochemical Aptamer-Based Biosensors for the Detection of Cardiac Biomarkers. ACS Omega, 2018, 3, 12010-12018.	3.5	111

#	Article	IF	CITATIONS
199	Reduced Graphene-Oxide-Embedded Polymeric Nanofiber Mats: An "On-Demand―Photothermally Triggered Antibiotic Release Platform. ACS Applied Materials & Interfaces, 2018, 10, 41098-41106.	8.0	75
200	Preparation of mussel-inspired perfluorinated polydopamine film on brass substrates: Superhydrophobic and anti-corrosion application. Progress in Organic Coatings, 2018, 125, 109-118.	3.9	29
201	Improved photodynamic effect through encapsulation of two photosensitizers in lipid nanocapsules. Journal of Materials Chemistry B, 2018, 6, 5949-5963.	5.8	15
202	Effect of cobalt addition on the corrosion behavior of near equiatomic NiTi shape memory alloy in normal saline solution: electrochemical and XPS studies. RSC Advances, 2018, 8, 19289-19300.	3.6	37
203	Sunlight-driven water-splitting using two-dimensional carbon based semiconductors. Journal of Materials Chemistry A, 2018, 6, 12876-12931.	10.3	215
204	Electrochemical Methodologies for the Detection of Pathogens. ACS Sensors, 2018, 3, 1069-1086.	7.8	178
205	Solution Processable Cu(II)macrocycle for the Formation of Cu <sub>2</sub> O Thin Film on Indium Tin Oxide and Its Application for Water Oxidation. Journal of Physical Chemistry C, 2018, 122, 16510-16518.	3.1	25
206	Enhanced antibacterial activity of carbon dots functionalized with ampicillin combined with visible light triggered photodynamic effects. Colloids and Surfaces B: Biointerfaces, 2018, 170, 347-354.	5.0	98
207	Graphene-Based Photocatalytic Materials for Conversion of Carbon Dioxide to Solar Fuels. , 2018, , 396-412.		2
208	Mesoporous silica nanoparticles in recent photodynamic therapy applications. Photochemical and Photobiological Sciences, 2018, 17, 1651-1674.	2.9	47
209	Heat: A Highly Efficient Skin Enhancer for Transdermal Drug Delivery. Frontiers in Bioengineering and Biotechnology, 2018, 6, 15.	4.1	79
210	Repeated photoporation with graphene quantum dots enables homogeneous labeling of live cells with extrinsic markers for fluorescence microscopy. Light: Science and Applications, 2018, 7, 47.	16.6	50
211	Fe-doped SnO2 decorated reduced graphene oxide nanocomposite with enhanced visible light photocatalytic activity. Journal of Photochemistry and Photobiology A: Chemistry, 2018, 367, 145-155.	3.9	26
212	Evaporation of nanofluid sessile drops: Infrared and acoustic methods to track the dynamic deposition of copper oxide nanoparticles. International Journal of Heat and Mass Transfer, 2018, 127, 1168-1177.	4.8	16
213	Porous Silicon Based Mass Spectrometry. , 2018, , 1-17.		0
214	Porous Silicon Based Mass Spectrometry. , 2018, , 1337-1353.		0
215	Surface Plasmon Resonance based sensing of lysozyme in serum on Micrococcus lysodeikticus-modified graphene oxide surfaces. Biosensors and Bioelectronics, 2017, 89, 525-531.	10.1	58
216	Label-free femtomolar cancer biomarker detection in human serum using graphene-coated surface plasmon resonance chips. Biosensors and Bioelectronics, 2017, 89, 606-611.	10.1	104

#	Article	IF	CITATIONS
217	Atomic Force Microscopic and Raman Investigation of Boron-Doped Diamond Nanowire Electrodes and Their Activity toward Oxygen Reduction. Journal of Physical Chemistry C, 2017, 121, 3397-3403.	3.1	13
218	Solvothermal synthesis of CoS/reduced porous graphene oxide nanocomposite for selective colorimetric detection of Hg(II) ion in aqueous medium. Sensors and Actuators B: Chemical, 2017, 244, 684-692.	7.8	80
219	Nickel oxide nanoparticles grafted on reduced graphene oxide (rGO/NiO) as efficient photocatalyst for reduction of nitroaromatics under visible light irradiation. Journal of Photochemistry and Photobiology A: Chemistry, 2017, 336, 198-207.	3.9	54
220	Co <sub>2</sub> SnO <sub>4</sub> nanoparticles as a high performance catalyst for oxidative degradation of rhodamine B dye and pentachlorophenol by activation of peroxymonosulfate. Physical Chemistry Chemical Physics, 2017, 19, 6569-6578.	2.8	48
221	Characterization of peptide attachment on silicon nanowires by X-ray photoelectron spectroscopy and mass spectrometry. Analyst, The, 2017, 142, 969-978.	3.5	10
222	Graphene-Microbial Interactions. , 2017, , 289-314.		0
223	3D silicon shapes through bulk nano structuration by focused ion beam implantation and wet etching. Nanotechnology, 2017, 28, 205301.	2.6	7
224	On demand electrochemical release of drugs from porous reduced graphene oxide modified flexible electrodes. Journal of Materials Chemistry B, 2017, 5, 6557-6565.	5.8	13
225	MoS2/TiO2/SiNW surface as an effective substrate for LDI-MS detection of glucose and glutathione in real samples. Talanta, 2017, 171, 101-107.	5.5	24
226	Core–shell structured reduced graphene oxide wrapped magnetically separable rGO@CuZnO@Fe3O4 microspheres as superior photocatalyst for CO2 reduction under visible light. Applied Catalysis B: Environmental, 2017, 205, 654-665.	20.2	111
227	Transdermal skin patch based on reduced graphene oxide: A new approach for photothermal triggered permeation of ondansetron across porcine skin. Journal of Controlled Release, 2017, 245, 137-146.	9.9	63
228	Facile synthesis of fluorinated polydopamine/chitosan/reduced graphene oxide composite aerogel for efficient oil/water separation. Chemical Engineering Journal, 2017, 326, 17-28.	12.7	255
229	Reduced graphene oxide as an efficient support for CdS-MoS2 heterostructures for enhanced photocatalytic H2 evolution. International Journal of Hydrogen Energy, 2017, 42, 16449-16458.	7.1	52
230	Short-term exposure to gold nanoparticle suspension impairs swimming behavior in a widespread calanoid copepod. Environmental Pollution, 2017, 228, 102-110.	7.5	12
231	Revealing the structure and functionality of graphene oxide and reduced graphene oxide/pyrene carboxylic acid interfaces by correlative spectral and imaging analysis. Physical Chemistry Chemical Physics, 2017, 19, 16038-16046.	2.8	22
232	Visible light assisted hydrogen generation from complete decomposition of hydrous hydrazine using rhodium modified TiO2 photocatalysts. Photochemical and Photobiological Sciences, 2017, 16, 1036-1042.	2.9	15
233	Carbon nanowalls: a new versatile graphene based interface for the laser desorption/ionization-mass spectrometry detection of small compounds in real samples. Nanoscale, 2017, 9, 9701-9715.	5.6	32
234	Electrophoretic Approach for the Simultaneous Deposition and Functionalization of Reduced Graphene Oxide Nanosheets with Diazonium Compounds: Application for Lysozyme Sensing in Serum. ACS Applied Materials & Interfaces, 2017, 9, 12823-12831.	8.0	31

#	Article	IF	CITATIONS
235	Reduced graphene oxide decorated with Co3O4 nanoparticles (rGO-Co3O4) nanocomposite: A reusable catalyst for highly efficient reduction of 4-nitrophenol, and Cr(VI) and dye removal from aqueous solutions. Chemical Engineering Journal, 2017, 322, 375-384.	12.7	160
236	Electrochemically stimulated drug release from flexible electrodes coated electrophoretically with doxorubicin loaded reduced graphene oxide. Chemical Communications, 2017, 53, 4022-4025.	4.1	36
237	Preparation of silver nanoparticles/polydopamine functionalized polyacrylonitrile fiber paper and its catalytic activity for the reduction 4-nitrophenol. Applied Surface Science, 2017, 411, 163-169.	6.1	67
238	MoS2/reduced graphene oxide nanocomposite for sensitive sensing of cysteamine in presence of uric acid in human plasma. Materials Science and Engineering C, 2017, 73, 627-632.	7.3	26
239	Facile synthesis of carbon-ZnO nanocomposite with enhanced visible light photocatalytic performance. Applied Surface Science, 2017, 400, 461-470.	6.1	67
240	Toxicity effect of graphene oxide on growth and photosynthetic pigment of the marine alga Picochlorum sp. during different growth stages. Environmental Science and Pollution Research, 2017, 24, 4144-4152.	5.3	57
241	Copper oxide supported on three-dimensional ammonia-doped porous reduced graphene oxide prepared through electrophoretic deposition for non-enzymatic glucose sensing. Electrochimica Acta, 2017, 224, 346-354.	5.2	53
242	Flexible Nanoholey Patches for Antibiotic-Free Treatments of Skin Infections. ACS Applied Materials & Interfaces, 2017, 9, 36665-36674.	8.0	42
243	Porous reduced graphene oxide modified electrodes for the analysis of protein aggregation. Part 1: Lysozyme aggregation at pH 2 and 7.4. Electrochimica Acta, 2017, 254, 375-383.	5.2	15
244	Nanomaterials for transdermal drug delivery: beyond the state of the art of liposomal structures. Journal of Materials Chemistry B, 2017, 5, 8653-8675.	5.8	62
245	Efficient and Durable Oxygen Reduction Electrocatalyst Based on CoMn Alloy Oxide Nanoparticles Supported Over N-Doped Porous Graphene. ACS Catalysis, 2017, 7, 6700-6710.	11.2	104
246	Functionalization of Reduced Graphene Oxide via Thiol–Maleimide "Click―Chemistry: Facile Fabrication of Targeted Drug Delivery Vehicles. ACS Applied Materials & Interfaces, 2017, 9, 34194-34203.	8.0	63
247	Selective isolation and eradication of E. coli associated with urinary tract infections using anti-fimbrial modified magnetic reduced graphene oxide nanoheaters. Journal of Materials Chemistry B, 2017, 5, 8133-8142.	5.8	23
248	Magnetic reduced graphene oxide loaded hydrogels: Highly versatile and efficient adsorbents for dyes and selective Cr(VI) ions removal. Journal of Colloid and Interface Science, 2017, 507, 360-369.	9.4	72
249	Room-Temperature Wet Chemical Synthesis of Au NPs/TiH2/Nanocarved Ti Self-Supported Electrocatalysts for Highly Efficient H2 Generation. ACS Applied Materials & Interfaces, 2017, 9, 30115-30126.	8.0	7
250	Advancements on the molecular design of nanoantibiotics: current level of development and future challenges. Molecular Systems Design and Engineering, 2017, 2, 349-369.	3.4	40
251	Controlled fabrication of NiO/ZnO superhydrophobic surface on zinc substrate with corrosion and abrasion resistance. Journal of Alloys and Compounds, 2017, 723, 225-236.	5.5	37
252	Substance P enhances lactic acid and tyramine production in Enterococcus faecalis V583 and promotes its cytotoxic effect on intestinal Caco-2/TC7 cells. Gut Pathogens, 2017, 9, 20.	3.4	10

#	Article	IF	CITATIONS
253	N-doped porous reduced graphene oxide as an efficient electrode material for high performance flexible solid-state supercapacitor. Applied Materials Today, 2017, 8, 141-149.	4.3	69
254	Photothermally triggered on-demand insulin release from reduced graphene oxide modified hydrogels. Journal of Controlled Release, 2017, 246, 164-173.	9.9	70
255	Cu-Ag bimetallic nanoparticles on reduced graphene oxide nanosheets as peroxidase mimic for glucose and ascorbic acid detection. Sensors and Actuators B: Chemical, 2017, 238, 842-851.	7.8	259
256	Polyurethane sponge functionalized with superhydrophobic nanodiamond particles for efficient oil/water separation. Chemical Engineering Journal, 2017, 307, 319-325.	12.7	237
257	Wilkinsonâ€Type Immobilized Catalyst on Diamond Nanoparticles for Alkene Reduction. ChemCatChem, 2017, 9, 432-439.	3.7	11
258	Enterocin B3A-B3B produced by LAB collected from infant faeces: potential utilization in the food industry for Listeria monocytogenes biofilm management. Antonie Van Leeuwenhoek, 2017, 110, 205-219.	1.7	35
259	Structural and optical properties of Na doped ZnO nanocrystals: Application to solar photocatalysis. Applied Surface Science, 2017, 396, 1528-1538.	6.1	99
260	Diamond Nanowires: A Recent Success Story for Biosensing. Springer Series on Chemical Sensors and Biosensors, 2017, , 1-18.	0.5	2
261	The multiple effects of organoclay and solvent evaporation on hydrophobicity of composite surfaces. Turkish Journal of Chemistry, 2017, 41, 793-801.	1.2	1
262	Comparison of Ti-Based Coatings on Silicon Nanowires for Phosphopeptide Enrichment and Their Laser Assisted Desorption/Ionization Mass Spectrometry Detection. Nanomaterials, 2017, 7, 272.	4.1	5
263	Effect of incubation duration, growth temperature, and abiotic surface type on cell surface properties, adhesion and pathogenicity of biofilm-detached Staphylococcus aureus cells. AMB Express, 2017, 7, 191.	3.0	27
264	Graphite oxide catalyzed synthesis of \$eta \$-amino alcohols by ring-opening of epoxides. Turkish Journal of Chemistry, 2017, 41, 70-79.	1.2	3
265	Differentiation of Crohn's Disease-Associated Isolates from Other Pathogenic Escherichia coli by Fimbrial Adhesion under Shear Force. Biology, 2016, 5, 14.	2.8	11
266	Oxidative Burst-Dependent NETosis Is Implicated in the Resolution of Necrosis-Associated Sterile Inflammation. Frontiers in Immunology, 2016, 7, 557.	4.8	55
267	Anti-MRSA Activities of Enterocins DD28 and DD93 and Evidences on Their Role in the Inhibition of Biofilm Formation. Frontiers in Microbiology, 2016, 7, 817.	3.5	54
268	Aptamer-Based Electrochemical Sensing of Lysozyme. Chemosensors, 2016, 4, 10.	3.6	43
269	Antibacterial Applications of Nanodiamonds. International Journal of Environmental Research and Public Health, 2016, 13, 413.	2.6	59
270	Nickel Decorated on Phosphorous-Doped Carbon Nitride as an Efficient Photocatalyst for Reduction of Nitrobenzenes. Nanomaterials, 2016, 6, 59.	4.1	121

#	Article	IF	CITATIONS
271	Non-Enzymatic Glucose Sensing Using Carbon Quantum Dots Decorated with Copper Oxide Nanoparticles. Sensors, 2016, 16, 1720.	3.8	40
272	Insulin impregnated reduced graphene oxide/Ni(OH)2 thin films for electrochemical insulin release and glucose sensing. Sensors and Actuators B: Chemical, 2016, 237, 693-701.	7.8	23
273	Synthesis and Functional Coating of Nanostructured Silicon as an Effective Substrate for Laser Desorption/Ionization Mass Spectrometry. Journal of Nanoscience and Nanotechnology, 2016, 16, 7994-7998.	0.9	1
274	Iron addition induced tunable band gap and tetravalent Fe ion in hydrothermally prepared SnO2 nanocrystals: Application in photocatalysis. Materials Research Bulletin, 2016, 83, 481-490.	5.2	37
275	Hydrothermal synthesis of ZTO/graphene nanocomposite with excellent photocatalytic activity under visible light irradiation. Journal of Colloid and Interface Science, 2016, 473, 66-74.	9.4	25
276	One-step synthesis of Au nanoparticle–graphene composites using tyrosine: electrocatalytic and catalytic properties. New Journal of Chemistry, 2016, 40, 5473-5482.	2.8	35
277	Green Synthesis of Reduced Graphene Oxide-Silver Nanoparticles Using Environmentally Friendly L-arginine for H <sub>2</sub> O <sub>2</sub> Detection. ECS Journal of Solid State Science and Technology, 2016, 5, M3060-M3066.	1.8	16
278	Nanodiamond–PMO for two-photon PDT and drug delivery. Journal of Materials Chemistry B, 2016, 4, 5803-5808.	5.8	49
279	A Prussian blue/carbon dot nanocomposite as an efficient visible light active photocatalyst for C-H activation of amines. Photochemical and Photobiological Sciences, 2016, 15, 1282-1288.	2.9	24
280	Antibacterial activity of graphene-based materials. Journal of Materials Chemistry B, 2016, 4, 6892-6912.	5.8	246
281	How the Intricate Interactions between Carbon Nanotubes and Two Bilirubin Oxidases Control Direct and Mediated O <sub>2</sub> Reduction. ACS Applied Materials & Interfaces, 2016, 8, 23074-23085.	8.0	91
282	High photocatalytic activity of plasmonic Ag@AgCl/Zn <sub>2</sub> SnO <sub>4</sub> nanocomposites synthesized using hydrothermal method. RSC Advances, 2016, 6, 80310-80319.	3.6	11
283	A 980 nm driven photothermal ablation of virulent and antibiotic resistant Gram-positive and Gram-negative bacteria strains using Prussian blue nanoparticles. Journal of Colloid and Interface Science, 2016, 480, 63-68.	9.4	53
284	Hydrothermal preparation of MoS2/TiO2/Si nanowires composite with enhanced photocatalytic performance under visible light. Materials and Design, 2016, 109, 634-643.	7.0	54
285	pHâ€responsive phenylboronic acidâ€modified diamond particles: Switch in carbohydrate capture ability triggers modulation of physicochemical and lectinâ€recognition properties. Physica Status Solidi (A) Applications and Materials Science, 2016, 213, 2124-2130.	1.8	2
286	Reduced Graphene Oxide Modified Electrodes for Sensitive Sensing of Gliadin in Food Samples. ACS Sensors, 2016, 1, 1462-1470.	7.8	57
287	Enhanced Photoluminescence in Acetylene-Treated ZnO Nanorods. Nanoscale Research Letters, 2016, 11, 413.	5.7	6
288	Carbon-Based Nanostructures for Matrix-Free Mass Spectrometry. Carbon Nanostructures, 2016, , 331-356.	0.1	2

#	Article	IF	CITATIONS
289	A quantitative method to discriminate between non-specific and specific lectin–glycan interactions on silicon-modified surfaces. Journal of Colloid and Interface Science, 2016, 464, 198-205.	9.4	3
290	Light-Triggered Release of Biomolecules from Diamond Nanowire Electrodes. Langmuir, 2016, 32, 6515-6523.	3.5	9
291	Cathodic activation of titanium-supported gold nanoparticles: An efficient and stable electrocatalyst for the hydrogen evolution reaction. International Journal of Hydrogen Energy, 2016, 41, 6326-6341.	7.1	36
292	MoS2/reduced graphene oxide as active hybrid material for the electrochemical detection of folic acid in human serum. Biosensors and Bioelectronics, 2016, 85, 807-813.	10.1	113
293	Affinity of Glycanâ€Modified Nanodiamonds towards Lectins and Uropathogenic <i>Escherichia Coli</i> . ChemNanoMat, 2016, 2, 307-314.	2.8	16
294	Preparation and characterization of Ni-doped ZnO–SnO2 nanocomposites: Application in photocatalysis. Superlattices and Microstructures, 2016, 91, 225-237.	3.1	43
295	Green chemistry approach for the synthesis of ZnO–carbon dots nanocomposites with good photocatalytic properties under visible light. Journal of Colloid and Interface Science, 2016, 465, 286-294.	9.4	137
296	Fabrication of stable homogeneous superhydrophobic HDPE/graphene oxide surfaces on zinc substrates. RSC Advances, 2016, 6, 29823-29829.	3.6	13
297	Electrophoretic Deposition of Carbon Nanofibers/Co(OH) <sub>2</sub> Nanocomposites: Application for Nonâ€Enzymatic Glucose Sensing. Electroanalysis, 2016, 28, 119-125.	2.9	34
298	Vertically Aligned Nitrogen-Doped Carbon Nanotube Carpet Electrodes: Highly Sensitive Interfaces for the Analysis of Serum from Patients with Inflammatory Bowel Disease. ACS Applied Materials & Interfaces, 2016, 8, 9600-9609.	8.0	16
299	High Efficiency of Functional Carbon Nanodots as Entry Inhibitors of Herpes Simplex Virus Type 1. ACS Applied Materials & Interfaces, 2016, 8, 9004-9013.	8.0	112
300	Eco-friendly synthesis of ZnO nanoparticles with different morphologies and their visible light photocatalytic performance for the degradation of Rhodamine B. Ceramics International, 2016, 42, 10259-10265.	4.8	116
301	Enhanced Ultraviolet Luminescence of ZnO Nanorods Treated by High-Pressure Water Vapor Annealing (HWA). Journal of Physical Chemistry C, 2016, 120, 4571-4580.	3.1	20
302	Ultrasound-assisted direct oxidative amidation of benzyl alcohols catalyzed by graphite oxide. Ultrasonics Sonochemistry, 2016, 32, 37-43.	8.2	28
303	Glucose-Derived Porous Carbon-Coated Silicon Nanowires as Efficient Electrodes for Aqueous Micro-Supercapacitors. ACS Applied Materials & Interfaces, 2016, 8, 4298-4302.	8.0	51
304	Electrochemically triggered release of drugs. European Polymer Journal, 2016, 83, 467-477.	5.4	44
305	Investigation of morphology, reflectance and photocatalytic activity of nanostructured silicon surfaces. Microelectronic Engineering, 2016, 159, 94-101.	2.4	12
306	Particle-based photodynamic therapy based on indocyanine green modified plasmonic nanostructures for inactivation of a Crohn's disease-associated Escherichia coli strain. Journal of Materials Chemistry B, 2016, 4, 2598-2605.	5.8	17

#	Article	IF	CITATIONS
307	Plasmonic photothermal cancer therapy with gold nanorods/reduced graphene oxide core/shell nanocomposites. RSC Advances, 2016, 6, 1600-1610.	3.6	70
308	Lipid nanocapsules for behavioural testing in aquatic toxicology: Time–response of Eurytemora affinis to environmental concentrations of PAHs and PCB. Aquatic Toxicology, 2016, 170, 310-322.	4.0	11
309	Reduction of Cr(VI) to Cr(III) using silicon nanowire arrays under visible light irradiation. Journal of Hazardous Materials, 2016, 304, 441-447.	12.4	41
310	Visible Light Assisted Photocatalytic [3 + 2] Azide–Alkyne "Click―Reaction for the Synthesis of 1,4-Substituted 1,2,3-Triazoles Using a Novel Bimetallic Ru–Mn Complex. ACS Sustainable Chemistry and Engineering, 2016, 4, 69-75.	6.7	56
311	Sulfonated reduced graphene oxide as a highly efficient catalyst for direct amidation of carboxylic acids with amines using ultrasonic irradiation. Ultrasonics Sonochemistry, 2016, 29, 371-379.	8.2	73
312	Detection of folic acid protein in human serum using reduced graphene oxide electrodes modified by folic-acid. Biosensors and Bioelectronics, 2016, 75, 389-395.	10.1	54
313	Cumulative effect of zinc oxide and titanium oxide nanoparticles on growth and chlorophyll a content of Picochlorum sp Environmental Science and Pollution Research, 2016, 23, 2821-2830.	5.3	66
314	Catalytic activity of silicon nanowires decorated with silver and copper nanoparticles. Semiconductor Science and Technology, 2016, 31, 014011.	2.0	16
315	Construction of a bone-like surface layer on hydroxyl-modified carbon/carbon composite implants via biomimetic mineralization and in vivo tests. RSC Advances, 2016, 6, 9370-9378.	3.6	7
316	Plasmonic Photothermal Therapy with Gold Nanorods/Reduced Graphene Oxide Core/Shell Nanocomposites. , 2016, , 3287-3294.		0
317	Combining combing and secondary ion mass spectrometry to study DNA on chips using 13C and 15N labeling. F1000Research, 2016, 5, 1437.	1.6	4
318	Selective Antimicrobial and Antibiofilm Disrupting Properties of Functionalized Diamond Nanoparticles Against <i>Escherichia coli</i> and <i>Staphylococcus aureus</i> . Particle and Particle Systems Characterization, 2015, 32, 822-830.	2.3	33
319	Surface Plasmon Resonance (SPR) for the Evaluation of Shear-Force-Dependent Bacterial Adhesion. Biosensors, 2015, 5, 276-287.	4.7	15
320	Nanostructures for the Inhibition of Viral Infections. Molecules, 2015, 20, 14051-14081.	3.8	104
321	Diamond Nanowires: A Novel Platform for Electrochemistry and Matrix-Free Mass Spectrometry. Sensors, 2015, 15, 12573-12593.	3.8	41
322	Unprecedented inhibition of glycosidase-catalyzed substrate hydrolysis by nanodiamond-grafted O-glycosides. RSC Advances, 2015, 5, 100568-100578.	3.6	27
323	A graphene/hemin hybrid material as an efficient green catalyst for stereoselective olefination of aldehydes. RSC Advances, 2015, 5, 100011-100017.	3.6	5
324	Dependence between the Refractive-Index Sensitivity of Metallic Nanoparticles and the Spectral Position of Their Localized Surface Plasmon Band: A Numerical and Analytical Study. Journal of Physical Chemistry C, 2015, 119, 28551-28559.	3.1	39

#	Article	IF	CITATIONS
325	Graphene Oxide Supported Molybdenum Cluster: First Heterogenized Homogeneous Catalyst for the Synthesis of Dimethylcarbonate from CO 2 and Methanol. Chemistry - A European Journal, 2015, 21, 3488-3494.	3.3	39
326	Antimicrobial activity of menthol modified nanodiamond particles. Diamond and Related Materials, 2015, 57, 2-8.	3.9	44
327	Preparation of reduced graphene oxide/Cu nanoparticle composites through electrophoretic deposition: application for nonenzymatic glucose sensing. RSC Advances, 2015, 5, 15861-15869.	3.6	100
328	Electrochemically triggered release of human insulin from an insulin-impregnated reduced graphene oxide modified electrode. Chemical Communications, 2015, 51, 14167-14170.	4.1	26
329	Hydrothermal synthesis, phase structure, optical and photocatalytic properties of Zn2SnO4 nanoparticles. Journal of Colloid and Interface Science, 2015, 457, 360-369.	9.4	65
330	Hexamolybdenum clusters supported on graphene oxide: Visible-light induced photocatalytic reduction of carbon dioxide into methanol. Carbon, 2015, 94, 91-100.	10.3	69
331	Palladium nanoparticles supported on reduced graphene oxide as an efficient catalyst for the reduction of benzyl alcohol compounds. Catalysis Communications, 2015, 69, 97-103.	3.3	29
332	Near-Field and Far-Field Sensitivities of LSPR Sensors. Journal of Physical Chemistry C, 2015, 119, 9470-9476.	3.1	23
333	Octahedral rhenium K4[Re6S8(CN)6] and Cu(OH)2 cluster modified TiO2 for the photoreduction of CO2 under visible light irradiation. Applied Catalysis A: General, 2015, 499, 32-38.	4.3	21
334	Plasmon waveguide resonance for sensing glycan–lectin interactions. Analytica Chimica Acta, 2015, 873, 71-79.	5.4	15
335	Inorganic Molybdenum Octahedral Nanosized Cluster Units, Versatile Functional Building Block for Nanoarchitectonics. Journal of Inorganic and Organometallic Polymers and Materials, 2015, 25, 189-204.	3.7	102
336	Controllable fabrication of stable superhydrophobic surfaces on iron substrates. RSC Advances, 2015, 5, 40657-40667.	3.6	19
337	Controllable growth of durable superhydrophobic coatings on a copper substrate via electrodeposition. Physical Chemistry Chemical Physics, 2015, 17, 10871-10880.	2.8	52
338	Cold–graphene nanocomposites for sensing and biomedical applications. Journal of Materials Chemistry B, 2015, 3, 4301-4324.	5.8	144
339	Infrared Photothermal Therapy with Water Soluble Reduced Graphene Oxide: Shape, Size and Reduction Degree Effects. Nano LIFE, 2015, 05, 1540002.	0.9	15
340	Carbohydrate Microarray for the Detection of Glycan–Protein Interactions Using Metal-Enhanced Fluorescence. Analytical Chemistry, 2015, 87, 3721-3728.	6.5	30
341	Toward Multifunctional "Clickable―Diamond Nanoparticles. Langmuir, 2015, 31, 3926-3933.	3.5	30
342	Effect of magnetic iron oxide (Fe3O4) nanoparticles on the growth and photosynthetic pigment content of Picochlorum sp Environmental Science and Pollution Research, 2015, 22, 11728-11739.	5.3	38

#	Article	IF	CITATIONS
343	Lipid nanocapsules containing the non-ionic surfactant Solutol HS15 inhibit the transport of calcium through hyperforin-activated channels in neuronal cells. Neuropharmacology, 2015, 99, 726-734.	4.1	11
344	Morphological and Optical Properties of Stain Etched Silicon in Vanadium Oxide (V2O5) / Hydrofluoric Acid (HF) Solution. ECS Transactions, 2015, 69, 87-93.	0.5	0
345	Reduced graphene oxide nanosheets decorated with AuPd bimetallic nanoparticles: a multifunctional material for photothermal therapy of cancer cells. Journal of Materials Chemistry B, 2015, 3, 8366-8374.	5.8	29
346	Magnetic Co <sub>3</sub> O <sub>4</sub> /reduced graphene oxide nanocomposite as a superior heterogeneous catalyst for one-pot oxidative esterification of aldehydes to methyl esters. RSC Advances, 2015, 5, 88567-88573.	3.6	22
347	Reduced graphene oxide nanosheets decorated with Au, Pd and Au–Pd bimetallic nanoparticles as highly efficient catalysts for electrochemical hydrogen generation. Journal of Materials Chemistry A, 2015, 3, 20254-20266.	10.3	146
348	A novel Ru/TiO <sub>2</sub> hybrid nanocomposite catalyzed photoreduction of CO <sub>2</sub> to methanol under visible light. Nanoscale, 2015, 7, 15258-15267.	5.6	55
349	Lipid nanocapsules as a new delivery system in copepods: Toxicity studies and optical imaging. Colloids and Surfaces B: Biointerfaces, 2015, 135, 441-447.	5.0	4
350	Highly effective photodynamic inactivation of E. coli using gold nanorods/SiO <sub>2</sub> core–shell nanostructures with embedded verteporfin. Chemical Communications, 2015, 51, 16365-16368.	4.1	25
351	Inhibition of type 1 fimbriae-mediated Escherichia coli adhesion and biofilm formation by trimeric cluster thiomannosides conjugated to diamond nanoparticles. Nanoscale, 2015, 7, 2325-2335.	5.6	52
352	Cobalt phthalocyanine tetracarboxylic acid modified reduced graphene oxide: a sensitive matrix for the electrocatalytic detection of peroxynitrite and hydrogen peroxide. RSC Advances, 2015, 5, 1474-1484.	3.6	70
353	Boronic acid-modified lipid nanocapsules: a novel platform for the highly efficient inhibition of hepatitis C viral entry. Nanoscale, 2015, 7, 1392-1402.	5.6	25
354	Ultrasound assisted direct oxidative esterification of aldehydes and alcohols using graphite oxide and Oxone. Ultrasonics Sonochemistry, 2015, 22, 359-364.	8.2	30
355	Influence of adsorption parameters of basic red dye 46 by the rough and treated Algerian natural phosphates. Journal of Industrial and Engineering Chemistry, 2015, 25, 229-238.	5.8	29
356	Plasmonic photothermal destruction of uropathogenic E. coli with reduced graphene oxide and core/shell nanocomposites of gold nanorods/reduced graphene oxide. Journal of Materials Chemistry B, 2015, 3, 375-386.	5.8	88
357	Plasmonic Photothermal Therapy with Gold Nanorods/Reduced Graphene Oxide Core/Shell Nanocomposites. , 2015, , 1-8.		1
358	CHAPTER 4. Peroxynitrite-Sensitive Electrochemically Active Matrices. RSC Detection Science, 2015, , 63-77.	0.0	0
359	Graphite oxide as an efficient solid reagent for esterification reactions. Turkish Journal of Chemistry, 2014, 38, 859-864.	1.2	20
360	Reduced Graphene Oxide Nanosheets Decorated with Au Nanoparticles as an Effective Bactericide: Investigation of Biocompatibility and Leakage of Sugars and Proteins. ChemPlusChem, 2014, 79, 1774-1784.	2.8	34

#	Article	IF	CITATIONS
361	Quantitative Assessment of the Multivalent Protein–Carbohydrate Interactions on Silicon. Analytical Chemistry, 2014, 86, 10340-10349.	6.5	20
362	Graphite oxide-promoted one-pot synthesis and oxidative aromatization of Hantzsch 1,4-dihydropyridines. Monatshefte Für Chemie, 2014, 145, 1919-1924.	1.8	14
363	Formation of nanostructured silicon surfaces by stain etching. Nanoscale Research Letters, 2014, 9, 482.	5.7	14
364	Micro-and nanostructured silicon-based superomniphobic surfaces. Journal of Colloid and Interface Science, 2014, 416, 280-288.	9.4	30
365	Carbohydrate–Lectin Interaction on Graphene-Coated Surface Plasmon Resonance (SPR) Interfaces. Plasmonics, 2014, 9, 677-683.	3.4	34
366	Palladium on activated carbon catalyzed reductive amination of aldehydes and ketones by triethylsilane. Applied Organometallic Chemistry, 2014, 28, 113-115.	3.5	20
367	Fabrication of superhydrophobic and highly oleophobic silicon-based surfaces via electroless etching method. Applied Surface Science, 2014, 295, 38-43.	6.1	20
368	Nanodiamond particles/reduced graphene oxide composites as efficient supercapacitor electrodes. Carbon, 2014, 68, 175-184.	10.3	69
369	Oxone/iron(II) sulfate/graphite oxide as a highly effective system for oxidation of alcohols under ultrasonic irradiation. Tetrahedron Letters, 2014, 55, 342-345.	1.4	28
370	Graphene-Coated Surface Plasmon Resonance Interfaces for Studying the Interactions between Bacteria and Surfaces. ACS Applied Materials & Interfaces, 2014, 6, 5422-5431.	8.0	65
371	Tip-Enhanced Raman Spectroscopy of Combed Double-Stranded DNA Bundles. Journal of Physical Chemistry C, 2014, 118, 1174-1181.	3.1	72
372	Photoreduction of CO2 to methanol with hexanuclear molybdenum [Mo6Br14]2â^' cluster units under visible light irradiation. RSC Advances, 2014, 4, 10420.	3.6	50
373	Preparation of reduced graphene oxide–Ni(OH) <sub>2</sub> composites by electrophoretic deposition: application for non-enzymatic glucose sensing. Journal of Materials Chemistry A, 2014, 2, 5525-5533.	10.3	128
374	Insulin loaded iron magnetic nanoparticle–graphene oxide composites: synthesis, characterization and application for in vivo delivery of insulin. RSC Advances, 2014, 4, 865-875.	3.6	33
375	Environmentally Friendly Reduction of Graphene Oxide Using Tyrosine for Nonenzymatic Amperometric H <sub>2</sub> O <sub>2</sub> Detection. Electroanalysis, 2014, 26, 156-163.	2.9	30
376	Porous Silicon-Based Mass Spectrometry. , 2014, , 1-16.		0
377	Biocompatibility of semiconducting silicon nanowires. , 2014, , 62-85.		4
378	Highly Sensitive Detection of DNA Hybridization on Commercialized Graphene-Coated Surface Plasmon Resonance Interfaces. Analytical Chemistry, 2014, 86, 11211-11216.	6.5	106

#	Article	IF	CITATIONS
379	Diamond nanowires modified with poly[3-(pyrrolyl)carboxylic acid] for the immobilization of histidine-tagged peptides. Analyst, The, 2014, 139, 4343.	3.5	8
380	Split and flow: reconfigurable capillary connection for digital microfluidic devices. Lab on A Chip, 2014, 14, 3589-3593.	6.0	18
381	Decoration of silicon nanostructures with copper particles for simultaneous selective capture and mass spectrometry detection of His-tagged model peptide. Analyst, The, 2014, 139, 5155-5163.	3.5	9
382	A convenient and efficient one-pot method for the synthesis of novel acridine-calix[4]arene derivatives as new DNA binding agents via multicomponent reaction. Supramolecular Chemistry, 2014, 26, 442-449.	1.2	11
383	Surface modification of semiconducting silicon nanowires for biosensing applications. , 2014, , 26-61.		8
384	Amplified plasmonic detection of DNA hybridization using doxorubicin-capped gold particles. Analyst, The, 2014, 139, 157-164.	3.5	26
385	An impedimetric immunosensor based on diamond nanowires decorated with nickel nanoparticles. Analyst, The, 2014, 139, 1726.	3.5	19
386	Graphite oxide: a simple and efficient solid acid catalyst for the ring-opening of epoxides by alcohols. Tetrahedron Letters, 2014, 55, 6694-6697.	1.4	44
387	Direct oxidative synthesis of nitrones from aldehydes and primary anilines using graphite oxide and Oxone. Tetrahedron Letters, 2014, 55, 5471-5474.	1.4	16
388	Surface plasmon resonance: signal amplification using colloidal gold nanoparticles for enhanced sensitivity. Reviews in Analytical Chemistry, 2014, 33, .	3.2	83
389	Lipid nanocapsules functionalized with polyethyleneimine for plasmid DNA and drug co-delivery and cell imaging. Nanoscale, 2014, 6, 7379.	5.6	24
390	Bioinspired Anchorable Thiol-Reactive Polymers: Synthesis and Applications Toward Surface Functionalization of Magnetic Nanoparticles. Macromolecules, 2014, 47, 5124-5134.	4.8	49
391	Production Rate and Reactivity of Singlet Oxygen1O2(1î"g) Directly Photoactivated at 1270 nm in Lipid Nanocapsules Dispersed in Water. Journal of Physical Chemistry C, 2014, 118, 2885-2893.	3.1	19
392	Enhancing LSPR Sensitivity of Au Gratings through Graphene Coupling to Au Film. Plasmonics, 2014, 9, 507-512.	3.4	44
393	Nitro-oxidative species in vivo biosensing: Challenges and advances with focus on peroxynitrite quantification. Biosensors and Bioelectronics, 2014, 58, 359-373.	10.1	48
394	Silicon Nanostructures-Graphene Nanocomposites. Advances in Chemical and Materials Engineering Book Series, 2014, , 176-195.	0.3	0
395	Metal Oxide-Graphene Nanocomposites. Advances in Chemical and Materials Engineering Book Series, 2014, , 196-225.	0.3	0
396	One-pot synthesis of 2-aminotetrahydrothiopyrano[4,3-b]pyran-3-carbonitrile derivatives using mesoporous NH2-MCM-41. Monatshefte FÃ1⁄4r Chemie, 2013, 144, 1699-1704.	1.8	6

#	Article	IF	CITATIONS
397	Amino-functionalized SBA-15 catalyzed one-step synthesis of 2-amino-5-cyano-4-hydroxy-6-aryl pyrimidines. Journal of the Iranian Chemical Society, 2013, 10, 559-563.	2.2	4
398	Non-enzymatic glucose sensing on long and short diamond nanowire electrodes. Electrochemistry Communications, 2013, 34, 286-290.	4.7	60
399	Lysozyme detection on aptamer functionalized graphene-coated SPR interfaces. Biosensors and Bioelectronics, 2013, 50, 239-243.	10.1	125
400	One-pot synthesis of gold nanoparticle/molybdenum cluster/graphene oxide nanocomposite and its photocatalytic activity. Applied Catalysis B: Environmental, 2013, 130-131, 270-276.	20.2	78
401	Search of Extremely Sensitive Near-Infrared Plasmonic Interfaces: A Theoretical Study. Plasmonics, 2013, 8, 1691-1698.	3.4	6
402	Clicking ferrocene to halogenated boron-doped diamond surfaces. Rare Metals, 2013, 32, 100-104.	7.1	1
403	Peroxynitrite activity of hemin-functionalized reduced graphene oxide. Analyst, The, 2013, 138, 4345.	3.5	42
404	Functionalization of Azide-Terminated Silicon Surfaces with Glycans Using Click Chemistry: XPS and FTIR Study. Journal of Physical Chemistry C, 2013, 117, 368-375.	3.1	81
405	Silica Cross-linked Micelles Loading with Silicon Nanoparticles: Preparation and Characterization. ACS Applied Materials & Interfaces, 2013, 5, 7042-7049.	8.0	18
406	Hypericin-loaded lipid nanocapsules for photodynamic cancer therapy in vitro. Nanoscale, 2013, 5, 10562.	5.6	45
407	Photochemical reaction of vitamin C with silicon nanocrystals: polymerization, hydrolysis and photoluminescence. Journal of Materials Chemistry C, 2013, 1, 5856.	5.5	6
408	Simultaneous electrochemical detection of tryptophan and tyrosine using boron-doped diamond and diamond nanowire electrodes. Electrochemistry Communications, 2013, 35, 84-87.	4.7	67
409	From micro to nano reentrant structures: hysteresis on superomniphobic surfaces. Colloid and Polymer Science, 2013, 291, 409-415.	2.1	39
410	Recent advances in surface chemistry strategies for the fabrication of functional iron oxide based magnetic nanoparticles. Nanoscale, 2013, 5, 10729.	5.6	164
411	Sensitive sugar detection using 4-aminophenylboronic acid modified graphene. Biosensors and Bioelectronics, 2013, 50, 331-337.	10.1	64
412	Cell micropatterning on superhydrophobic diamond nanowires. Acta Biomaterialia, 2013, 9, 4585-4591.	8.3	29
413	Electro-(de)wetting on Superhydrophobic Surfaces. Langmuir, 2013, 29, 13346-13351.	3.5	41
414	Preparation and Characterization of Decyl-Terminated Silicon Nanoparticles Encapsulated in Lipid Nanocapsules. Langmuir, 2013, 29, 12688-12696.	3.5	17

#	Article	IF	CITATIONS
415	Acoustic Tracking of Cassie to Wenzel Wetting Transitions. Langmuir, 2013, 29, 13129-13134.	3.5	32
416	The antimicrobial effect of silicon nanowires decorated with silver and copper nanoparticles. Nanotechnology, 2013, 24, 495101.	2.6	85
417	Phenylboronic-Acid-Modified Nanoparticles: Potential Antiviral Therapeutics. ACS Applied Materials & Interfaces, 2013, 5, 12488-12498.	8.0	71
418	Electroless chemical etching of silicon in aqueous NH4F/AgNO3/HNO3 solution. Applied Surface Science, 2013, 284, 894-899.	6.1	17
419	Investigation of the anti-biofouling properties of graphene oxide aqueous solutions by electrowetting characterization. Journal of Materials Chemistry A, 2013, 1, 12355.	10.3	8
420	Enhanced gold film-coupled graphene-based plasmonic nanosensor. Proceedings of SPIE, 2013, , .	0.8	0
421	Alkyl passivation and SiO2 encapsulation of silicon nanoparticles: preparation, surface modification and luminescence properties. Journal of Materials Chemistry C, 2013, 1, 5261.	5.5	13
422	Droplet based lab-on-chip microfluidic Microsystems integrated nanostructured surfaces for high sensitive mass spectrometry analysis. , 2013, , .		0
423	Recent advances in the development of graphene-based surface plasmon resonance (SPR) interfaces. Analytical and Bioanalytical Chemistry, 2013, 405, 1435-1443.	3.7	191
424	Comparison of photo- and Cu( <scp>i</scp> )-catalyzed "click―chemistries for the formation of carbohydrate SPR interfaces. Analyst, The, 2013, 138, 805-812.	3.5	32
425	Iron oxide magnetic nanoparticles with versatile surface functions based on dopamine anchors. Nanoscale, 2013, 5, 2692.	5.6	114
426	Palladium(II) acetate atalyzed reduction of imines to the corresponding amines by triethylsilane. Applied Organometallic Chemistry, 2013, 27, 174-176.	3.5	6
427	Electrowetting on functional fibers. Soft Matter, 2013, 9, 492-497.	2.7	14
428	Glycan-functionalized diamond nanoparticles as potent E. coli anti-adhesives. Nanoscale, 2013, 5, 2307.	5.6	102
429	Convenient and Efficient One-Pot Method for the Synthesis of 2-Amino-tetrahydro-4 <i>H</i> -chromenes and 2-Amino-4 <i>H</i> -benzo[ <i>h</i> ]-chromenes Using Catalytic Amount of Amino-Functionalized MCM-41 in Aqueous Media. Synthetic Communications, 2013, 43, 1499-1507.	2.1	45
430	The synthesis of citrate-modified silver nanoparticles in an aqueous suspension of graphene oxide nanosheets and their antibacterial activity. Colloids and Surfaces B: Biointerfaces, 2013, 105, 128-136.	5.0	137
431	Nanometal plasmonpolaritons. Surface Science Reports, 2013, 68, 1-67.	7.2	31
432	Effect of surface roughness and chemical composition on the wetting properties of silicon-based substrates. Comptes Rendus Chimie, 2013, 16, 65-72.	0.5	50

#	Article	IF	CITATIONS
433	Thiol–Yne Click Reactions on Alkynyl–Dopamineâ€Modified Reduced Graphene Oxide. Chemistry - A European Journal, 2013, 19, 8673-8678.	3.3	36
434	Diamond nanowires decorated with metallic nanoparticles: A novel electrical interface for the immobilization of histidinylated biomolecuels. Electrochimica Acta, 2013, 110, 4-8.	5.2	20
435	Approach for Plasmonic Based DNA Sensing: Amplification of the Wavelength Shift and Simultaneous Detection of the Plasmon Modes of Gold Nanostructures. Analytical Chemistry, 2013, 85, 3288-3296.	6.5	56
436	Voltammetric detection of l-dopa and carbidopa on graphene modified glassy carbon interfaces. Bioelectrochemistry, 2013, 93, 15-22.	4.6	37
437	Ferromagnetism induced in ZnO nanorods by morphology changes under a nitrogen–carbon atmosphere. RSC Advances, 2013, 3, 12945.	3.6	9
438	Droplet transport by electrowetting: lets get rough!. Microfluidics and Nanofluidics, 2013, 15, 327-336.	2.2	13
439	Functionalization of diamond surfaces for medical applications. , 2013, , 25-47.		4
440	Fabrication of silicon nanostructures using metalâ€assisted etching in NaBF <sub>4</sub> . Physica Status Solidi (A) Applications and Materials Science, 2013, 210, 2178-2182.	1.8	7
441	Characterization of the state of a droplet on a micro-textured silicon wafer using ultrasound. Journal of Applied Physics, 2012, 112, .	2.5	16
442	Dielectric coated plasmonic interfaces: their interest for sensitive sensing of analyte-ligand interactions. Reviews in Analytical Chemistry, 2012, 31, .	3.2	31
443	Sensing using localised surface plasmon resonance sensors. Chemical Communications, 2012, 48, 8999.	4.1	266
444	Vertical arrays of SiNWs–ZnO nanostructures as high performance electron field emitters. Journal of Materials Chemistry, 2012, 22, 22922.	6.7	23
445	Preparation and photocatalytic properties of quartz/gold nanostructures/TiO2 lamellar structures. RSC Advances, 2012, 2, 12482.	3.6	4
446	Nanomolar Hydrogen Peroxide Detection Using Horseradish Peroxidase Covalently Linked to Undoped Nanocrystalline Diamond Surfaces. Langmuir, 2012, 28, 587-592.	3.5	48
447	Plasmonic Nanoparticles Array for High-Sensitivity Sensing: A Theoretical Investigation. Journal of Physical Chemistry C, 2012, 116, 17819-17827.	3.1	30
448	Direct Characterization of Native Chemical Ligation of Peptides on Silicon Nanowires. Langmuir, 2012, 28, 13336-13344.	3.5	10
449	Graphite oxide: an efficient reagent for oxidation of alcohols under sonication. Tetrahedron Letters, 2012, 53, 4962-4965.	1.4	58
450	Reduction and Functionalization of Graphene Oxide Sheets Using Biomimetic Dopamine Derivatives in One Step. ACS Applied Materials & Interfaces, 2012, 4, 1016-1020.	8.0	182

#	Article	IF	CITATIONS
451	Lithographically patterned silicon nanostructures on silicon substrates. Applied Surface Science, 2012, 258, 6007-6012.	6.1	10
452	Laser desorption ionization mass spectrometry of protein tryptic digests on nanostructured silicon plates. Journal of Proteomics, 2012, 75, 1973-1990.	2.4	32
453	Diamond nanowires for highly sensitive matrix-free mass spectrometry analysis of small molecules. Nanoscale, 2012, 4, 231-238.	5.6	75
454	Investigation of Silicon-Based Nanostructure Morphology and Chemical Termination on Laser Desorption Ionization Mass Spectrometry Performance. Analytical Chemistry, 2012, 84, 10637-10644.	6.5	42
455	Preparation of graphene/tetrathiafulvalene nanocomposite switchable surfaces. Chemical Communications, 2012, 48, 1221-1223.	4.1	59
456	Sliding Droplets on Superomniphobic Zinc Oxide Nanostructures. Langmuir, 2012, 28, 389-395.	3.5	48
457	Affinity surface-assisted laser desorption/ionization mass spectrometry for peptide enrichment. Analyst, The, 2012, 137, 5527.	3.5	23
458	Surface-assisted laser desorption–ionization mass spectrometry on titanium dioxide (TiO2) nanotube layers. Analyst, The, 2012, 137, 3058.	3.5	41
459	Thiol-yne Reaction on Boron-Doped Diamond Electrodes: Application for the Electrochemical Detection of DNA–DNA Hybridization Events. Analytical Chemistry, 2012, 84, 194-200.	6.5	55
460	Inhibiting protein biofouling using graphene oxide in droplet-based microfluidic microsystems. Lab on A Chip, 2012, 12, 1601.	6.0	25
461	Preparation of a Responsive Carbohydrate-Coated Biointerface Based on Graphene/Azido-Terminated Tetrathiafulvalene Nanohybrid Material. ACS Applied Materials & Interfaces, 2012, 4, 5386-5393.	8.0	44
462	Zipping Effect on Omniphobic Surfaces for Controlled Deposition of Minute Amounts of Fluid or Colloids. Small, 2012, 8, 1229-1236.	10.0	74
463	Graphene-based high-performance surface plasmon resonance biosensors. Proceedings of SPIE, 2012, , .	0.8	8
464	Simple and low-cost fabrication of PDMS microfluidic round channels by surface-wetting parameters optimization. Microfluidics and Nanofluidics, 2012, 12, 953-961.	2.2	12
465	Fast photocatalytic degradation of rhodamine B over [Mo6Br8(N3)6]2â^' cluster units under sun light irradiation. Applied Catalysis B: Environmental, 2012, 123-124, 1-8.	20.2	75
466	Investigation of the corrosion behaviour of steel coated with amorphous silicon carbon alloys. Surface and Coatings Technology, 2012, 206, 3626-3631.	4.8	4
467	Graphite oxide mediated oxidative aromatization of 1,4-dihydropyridines into pyridine derivatives. Tetrahedron Letters, 2012, 53, 2473-2475.	1.4	51
468	Contact angle hysteresis origins: Investigation on super-omniphobic surfaces. Soft Matter, 2011, 7, 9380.	2.7	65

#	Article	IF	CITATIONS
469	Localized surface plasmon resonance interfaces coated with poly[3-(pyrrolyl)carboxylic acid] for histidine-tagged peptide sensing. Analyst, The, 2011, 136, 4211.	3.5	5
470	Plasmonic properties of silver nanostructures coated with an amorphous silicon–carbon alloy and their applications for sensitive sensing of DNA hybridization. Analyst, The, 2011, 136, 1859.	3.5	12
471	EWOD driven cleaning of bioparticles on hydrophobic and superhydrophobic surfaces. Lab on A Chip, 2011, 11, 490-496.	6.0	80
472	Combed Single DNA Molecules Imaged by Secondary Ion Mass Spectrometry. Analytical Chemistry, 2011, 83, 6940-6947.	6.5	27
473	Photocatalytic activity of silicon nanowires under UV and visible light irradiation. Chemical Communications, 2011, 47, 991-993.	4.1	65
474	Synthesis and photocatalytic activity of iodine-doped ZnO nanoflowers. Journal of Materials Chemistry, 2011, 21, 10982.	6.7	71
475	High sensitive matrix-free mass spectrometry analysis of peptides using silicon nanowires-based digital microfluidic device. Lab on A Chip, 2011, 11, 1620.	6.0	74
476	Development of a Metal-Chelated Plasmonic Interface for the Linking of His-Peptides with a Droplet-Based Surface Plasmon Resonance Read-Off Scheme. Langmuir, 2011, 27, 5498-5505.	3.5	25
477	Culture of mammalian cells on patterned superhydrophilic/superhydrophobic silicon nanowire arrays. Soft Matter, 2011, 7, 8642.	2.7	109
478	Optical and electrochemical properties of tunable host–guest complexes linked to plasmonic interfaces. Journal of Materials Chemistry, 2011, 21, 3006.	6.7	19
479	Surface plasmon resonance-based biosensors: From the development of different SPR structures to novel surface functionalization strategies. Current Opinion in Solid State and Materials Science, 2011, 15, 208-224.	11.5	295
480	Silicon nanowire arrays-induced graphene oxide reduction under UV irradiation. Nanoscale, 2011, 3, 4662.	5.6	71
481	Amino-Functionalized MCM-41 base-Catalyzed one-Pot synthesis of 2-Amino-5,6-dihydropyrimidin-4(3H)-ones. Journal of the Iranian Chemical Society, 2011, 8, 280-286.	2.2	12
482	Palladium chloride-catalyzed reductive cleavage of benzylic acetal, ketal and ether compounds with triethylsilane. Journal of the Iranian Chemical Society, 2011, 8, 570-573.	2.2	4
483	Preparation and characterization of Zonyl-coated nanodiamonds with antifouling properties. Chemical Communications, 2011, 47, 5178.	4.1	21
484	Direct Functionalization of Nanodiamond Particles Using Dopamine Derivatives. Langmuir, 2011, 27, 12451-12457.	3.5	94
485	Characterization of single transition metal oxide nanorods by combining atomic force microscopy and polarized micro-Raman spectroscopy. Chemical Physics Letters, 2011, 514, 128-133.	2.6	9
486	Preparation and electrochemical behaviour of PPy–CdS composite films. Journal of Electroanalytical Chemistry, 2011, 650, 176-181.	3.8	34

#	Article	IF	CITATIONS
487	Investigation of the corrosion behavior of carbon steel coated with fluoropolymer thin films. Surface and Coatings Technology, 2011, 205, 4011-4017.	4.8	37
488	Electrosynthesis and analysis of the electrochemical properties of a composite material: Polyaniline + titanium oxide. Thin Solid Films, 2011, 519, 3596-3602.	1.8	20
489	Theoretical and experimental study of the short and long range sensing using gold nanostructures. , 2010, , .		2
490	Matrix-Free Laser Desorption/Ionization Mass Spectrometry on Silicon Nanowire Arrays Prepared by Chemical Etching of Crystalline Silicon. Langmuir, 2010, 26, 1354-1361.	3.5	118
491	Covalent modification of boron-doped diamond electrodes with an imidazolium-based ionic liquid. Electrochimica Acta, 2010, 55, 1582-1587.	5.2	23
492	Palladium atalyzed reduction of nitroaromatic compounds to the corresponding anilines. Applied Organometallic Chemistry, 2010, 24, 477-480.	3.5	10
493	Covalent grafting of polyaniline onto aniline-terminated porous silicon. Optical Materials, 2010, 32, 748-752.	3.6	22
494	Amorphous silicon–carbon alloys for efficient localized surface plasmon resonance sensing. Biosensors and Bioelectronics, 2010, 25, 1199-1203.	10.1	26
495	Investigation of the corrosion protection of SiOx-like oxide films deposited by plasma-enhanced chemical vapor deposition onto carbon steel. Electrochimica Acta, 2010, 55, 8921-8927.	5.2	27
496	Molecular monolayers on silicon as substrates for biosensors. Bioelectrochemistry, 2010, 80, 17-25.	4.6	32
497	Localized surface plasmon-enhanced fluorescence spectroscopy for highly-sensitive real-time detection of DNA hybridization. Biosensors and Bioelectronics, 2010, 25, 2579-2585.	10.1	59
498	Distinction between surface hydroxyl and ether groups on boron-doped diamond electrodes using a chemical approach. Electrochemistry Communications, 2010, 12, 351-354.	4.7	48
499	Preparation of boron-doped diamond nanowires and their application for sensitive electrochemical detection of tryptophan. Electrochemistry Communications, 2010, 12, 438-441.	4.7	101
500	Preparation and reactivity of carboxylic acid-terminated boron-doped diamond electrodes. Electrochimica Acta, 2010, 55, 959-964.	5.2	5
501	Chemical and electrochemical grafting of polyaniline on anilineâ€ŧerminated porous silicon. Surface and Interface Analysis, 2010, 42, 1342-1346.	1.8	16
502	Electrochemical grafting of poly(3â€hexylthiophene) on porous silicon for gas sensing. Surface and Interface Analysis, 2010, 42, 1041-1045.	1.8	22
503	Comparison of different oxidation techniques on single-crystal and nanocrystalline diamond surfaces. Diamond and Related Materials, 2010, 19, 474-478.	3.9	57
504	HREELS Investigation of the Surfaces of Nanocrystalline Diamond Films Oxidized by Different Processes. Langmuir, 2010, 26, 18798-18805.	3.5	37

#	Article	IF	CITATIONS
505	Development of New Localized Surface Plasmon Resonance Interfaces Based on Gold Nanostructures Sandwiched between Tin-Doped Indium Oxide Films. Langmuir, 2010, 26, 4266-4273.	3.5	18
506	Label-Free Detection of Lectins on Carbohydrate-Modified Boron-Doped Diamond Surfaces. Analytical Chemistry, 2010, 82, 8203-8210.	6.5	66
507	Photochemical Immobilization of Proteins and Peptides on Benzophenone-Terminated Boron-Doped Diamond Surfaces. Langmuir, 2010, 26, 1075-1080.	3.5	30
508	Sensitivity of Plasmonic Nanostructures Coated with Thin Oxide Films for Refractive Index Sensing: Experimental and Theoretical Investigations. Journal of Physical Chemistry C, 2010, 114, 11769-11775.	3.1	37
509	Cell Adhesion Properties on Chemically Micropatterned Boron-Doped Diamond Surfaces. Langmuir, 2010, 26, 15065-15069.	3.5	18
510	Development and Characterization of a Diamond-Based Localized Surface Plasmon Resonance Interface. Journal of Physical Chemistry C, 2010, 114, 3346-3353.	3.1	33
511	Selective Adhesion of <i>Bacillus cereus</i> Spores on Heterogeneously Wetted Silicon Nanowires. Langmuir, 2010, 26, 3479-3484.	3.5	50
512	Engineering Sticky Superomniphobic Surfaces on Transparent and Flexible PDMS Substrate. Langmuir, 2010, 26, 17242-17247.	3.5	83
513	Chips from Chips: Application to the Study of Antibody Responses to Methylated Proteins. Journal of Proteome Research, 2010, 9, 6467-6478.	3.7	21
514	Functionalization of Diamond Nanoparticles Using "Click―Chemistry. Langmuir, 2010, 26, 13168-13172.	3.5	71
515	Stacking Faults-Induced Quenching of the UV Luminescence in ZnO. Journal of Physical Chemistry Letters, 2010, 1, 3033-3038.	4.6	37
516	Surface Plasmon-Enhanced Fluorescence Spectroscopy on Silver Based SPR Substrates. Journal of Physical Chemistry C, 2010, 114, 22582-22589.	3.1	33
517	Quantitative Testing of Robustness on Superomniphobic Surfaces by Drop Impact. Langmuir, 2010, 26, 18369-18373.	3.5	102
518	Surface Plasmon Resonance on Gold and Silver Films Coated with Thin Layers of Amorphous Siliconâ^'Carbon Alloys. Langmuir, 2010, 26, 6058-6065.	3.5	37
519	Cellular and in vivo toxicity of functionalized nanodiamond in Xenopus embryos. Journal of Materials Chemistry, 2010, 20, 8064.	6.7	98
520	Template assisted highly ordered novel self assembly of micro-reservoirs and its replication. Lab on A Chip, 2010, 10, 1902.	6.0	0
521	Preparation of superhydrophobic and oleophobic diamond nanograss array. Journal of Materials Chemistry, 2010, 20, 10671.	6.7	44
522	Electrowetting and droplet impalement experiments on superhydrophobic multiscale structures. Faraday Discussions, 2010, 146, 125.	3.2	33

#	Article	IF	CITATIONS
523	In Situ Chemical Modification of Peptide Microarrays: Characterization by Desorption/Ionization on Silicon Nanowires. Methods in Molecular Biology, 2010, 669, 125-133.	0.9	2
524	The collagen assisted self-assembly of silicon nanowires. Nanotechnology, 2009, 20, 235601.	2.6	14
525	Localized Surface Plasmon Resonance of Gold Nanoparticle-Modified Chitosan Films for Heavy-Metal Ions Sensing. Journal of Nanoscience and Nanotechnology, 2009, 9, 350-357.	0.9	18
526	Electro-oxidative nanopatterning of silane monolayers on boron-doped diamond electrodes. Nanotechnology, 2009, 20, 075302.	2.6	9
527	Me <sub>3</sub> SiCl and Et <sub>3</sub> Silâ€promoted oneâ€pot synthesis of 1,4â€dihydropyridine derivatives. Applied Organometallic Chemistry, 2009, 23, 267-271.	3.5	11
528	A simple and efficient hydrogenation of benzyl alcohols to methylene compounds using triethylsilane and a palladium catalyst. Tetrahedron Letters, 2009, 50, 5930-5932.	1.4	49
529	Formation of aligned silicon nanowire on silicon by electroless etching in HF solution. Journal of Luminescence, 2009, 129, 1750-1753.	3.1	24
530	Au-assisted electroless etching of silicon in aqueous HF/H2O2 solution. Applied Surface Science, 2009, 255, 6210-6216.	6.1	56
531	Electrochemical impedance spectroscopy of ZnO nanostructures. Electrochemistry Communications, 2009, 11, 945-949.	4.7	53
532	Comparison of the chemical composition of boron-doped diamond surfaces upon different oxidation processes. Electrochimica Acta, 2009, 54, 5818-5824.	5.2	79
533	Preparation and Characterization of Silver Substrates Coated with Antimony-Doped SnO <sub>2</sub> Thin Films for Surface Plasmon Resonance Studies. Langmuir, 2009, 25, 8036-8041.	3.5	33
534	"Clicking―Thiophene on Diamond Interfaces. Preparation of a Conducting Polythiophene/Diamond Hybrid Material. Journal of Physical Chemistry C, 2009, 113, 17082-17086.	3.1	27
535	Reversible Electrowetting on Superhydrophobic Double-Nanotextured Surfaces. Langmuir, 2009, 25, 6551-6558.	3.5	55
536	Preparation of Superhydrophobic Coatings on Zinc as Effective Corrosion Barriers. ACS Applied Materials & Interfaces, 2009, 1, 1150-1153.	8.0	285
537	Wet Chemical Approaches for Chemical Functionalization of Semiconductor Nanostructures. Nanostructure Science and Technology, 2009, , 183-248.	0.1	9
538	Preparation of Superhydrophobic Coatings on Zinc, Silicon, and Steel by a Solution-Immersion Technique. ACS Applied Materials & amp; Interfaces, 2009, 1, 2086-2091.	8.0	78
539	Silicon Nanowires Coated with Silver Nanostructures as Ultrasensitive Interfaces for Surface-Enhanced Raman Spectroscopy. ACS Applied Materials & Interfaces, 2009, 1, 1396-1403.	8.0	133
540	Synthesis and Luminescence Properties of (N-Doped) ZnO Nanostructures from a Dimethylformamide Aqueous Solution. Journal of Physical Chemistry C, 2009, 113, 13643-13650.	3.1	50

#	Article	IF	CITATIONS
541	Cheap and Efficient Protocol for the Synthesis of Tetrahydroquinazolinone, Dihydropyrimidinone, and Pyrimidinone Derivatives. Synthetic Communications, 2009, 40, 8-20.	2.1	11
542	Selective detection of hexachromium ions by localized surface plasmon resonance measurements using gold nanoparticles/chitosan composite interfaces. Analyst, The, 2009, 134, 881.	3.5	40
543	Short- and Long-Range Sensing Using Plasmonic Nanostrucures: Experimental and Theoretical Studies. Journal of Physical Chemistry C, 2009, 113, 15921-15927.	3.1	43
544	Clicking ferrocene groups to boron-doped diamond electrodes. Chemical Communications, 2009, , 2753.	4.1	42
545	Surface and Superlattice. Nanostructure Science and Technology, 2009, , 71-102.	0.1	0
546	Formation of aligned silicon-nanowire on silicon in aqueous HF/(AgNO3+Na2S2O8) solution. Applied Surface Science, 2008, 254, 7219-7222.	6.1	24
547	Preparation and characterization of thin organosilicon films deposited on SPR chip. Electrochimica Acta, 2008, 53, 3910-3915.	5.2	10
548	Different strategies for functionalization of diamond surfaces. Journal of Solid State Electrochemistry, 2008, 12, 1205-1218.	2.5	180
549	Efficient method for the reduction of carbonyl compounds by triethylsilane catalyzed by PdCl2. Journal of Organometallic Chemistry, 2008, 693, 3567-3570.	1.8	26
550	Investigation of the electrocatalytic activity of boron-doped diamond electrodes modified with palladium or gold nanoparticles for oxygen reduction reaction in basic medium. Comptes Rendus Chimie, 2008, 11, 1004-1009.	0.5	19
551	Preparation and characterization of antimony-doped SnO2 thin films on gold and silver substrates for electrochemical and surface plasmon resonance studies. Electrochemistry Communications, 2008, 10, 1041-1043.	4.7	24
552	Influence of the surface termination on the electrochemical properties of boron-doped diamond (BDD) interfaces. Electrochemistry Communications, 2008, 10, 402-406.	4.7	58
553	Seed-mediated electrochemical growth of gold nanostructures on indium tin oxide thin films. Electrochimica Acta, 2008, 53, 7838-7844.	5.2	42
554	Electrochemical investigation of the influence of thin SiOx films deposited on gold on charge transfer characteristics. Electrochimica Acta, 2008, 53, 7908-7914.	5.2	10
555	Short- and Long-Range Sensing on Gold Nanostructures, Deposited on Glass, Coated with Silicon Oxide Films of Different Thicknesses. Journal of Physical Chemistry C, 2008, 112, 8239-8243.	3.1	55
556	Gold island films on indium tin oxide for localized surface plasmon sensing. Nanotechnology, 2008, 19, 195712.	2.6	84
557	Application of Thin Titanium/Titanium Oxide Layers Deposited on Gold for Infrared Reflection Absorption Spectroscopy: Structural Studies of Lipid Bilayers. Langmuir, 2008, 24, 7378-7387.	3.5	19
558	Extreme Resistance of Superhydrophobic Surfaces to Impalement: Reversible Electrowetting Related to the Impacting/Bouncing Drop Test. Langmuir, 2008, 24, 11203-11208.	3.5	82

#	Article	IF	CITATIONS
559	Functionalization of Glassy Carbon with Diazonium Salts in Ionic Liquids. Langmuir, 2008, 24, 6327-6333.	3.5	47
560	Solvent-free chemical functionalization of hydrogen-terminated boron-doped diamond electrodes with diazonium salts in ionic liquids. Diamond and Related Materials, 2008, 17, 1394-1398.	3.9	10
561	Wet-chemical approach for the halogenation of hydrogenated boron-doped diamond electrodes. Chemical Communications, 2008, , 6294.	4.1	10
562	Thin chitosan films as a platform for SPR sensing of ferric ions. Analyst, The, 2008, 133, 673.	3.5	48
563	Preparation of Electrochemical and Surface Plasmon Resonance Active Interfaces: Deposition of Indium Tin Oxide on Silver Thin Films. Journal of Physical Chemistry C, 2008, 112, 10883-10888.	3.1	25
564	Polarization Modulation Infrared Reflection Absorption Spectroscopy Investigations of Thin Silica Films Deposited on Gold. 2. Structural Analysis of a 1,2-Dimyristoyl- <i>sn</i> -glycero-3-phosphocholine Bilayer. Langmuir, 2008, 24, 3922-3929.	3.5	34
565	Surface Plasmon Resonance Investigation of Silver and Gold Films Coated with Thin Indium Tin Oxide Layers: Influence on Stability and Sensitivity. Journal of Physical Chemistry C, 2008, 112, 15813-15817.	3.1	76
566	Microwave Effects on Chemical Functionalization of Hydrogen-Terminated Porous Silicon Nanostructures. Journal of Physical Chemistry C, 2008, 112, 16622-16628.	3.1	35
567	Biomolecule and Nanoparticle Transfer on Patterned and Heterogeneously Wetted Superhydrophobic Silicon Nanowire Surfaces. Langmuir, 2008, 24, 1670-1672.	3.5	69
568	Growth of Si nanowires on micropillars for the study of their dopant distribution by atom probe tomography. Journal of Vacuum Science & Technology B, 2008, 26, 1960-1963.	1.3	35
569	Electrochemical impedance spectroscopy and surface plasmon resonance studies of DNA hybridization on gold/SiOx interfaces. Analyst, The, 2008, 133, 1097.	3.5	39
570	Preparation of Superhydrophobic Silicon Oxide Nanowire Surfaces. Langmuir, 2007, 23, 1608-1611.	3.5	111
571	Photografting and patterning of oligonucleotides on benzophenone-modified boron-doped diamond. Chemical Communications, 2007, , 2793.	4.1	24
572	Peptide Immobilization on Amine-Terminated Boron-Doped Diamond Surfaces. Langmuir, 2007, 23, 4494-4497.	3.5	38
573	Influence of the Surface Termination of Boron-Doped Diamond Electrodes on Oxygen Reduction in Basic Medium. Electrochemical and Solid-State Letters, 2007, 10, G43.	2.2	29
574	PM IRRAS Investigation of Thin Silica Films Deposited on Gold. Part 1. Theory and Proof of Concept. Langmuir, 2007, 23, 9303-9309.	3.5	32
575	Reversible Electrowetting on Superhydrophobic Silicon Nanowires. Nano Letters, 2007, 7, 813-817.	9.1	225
576	Covalent linking of peptides onto oxygen-terminated boron-doped diamond surfaces. Diamond and Related Materials, 2007, 16, 892-898.	3.9	29

#	Article	IF	CITATIONS
577	Covalent functionalization of silicon nitride surfaces by semicarbazide group. Surface Science, 2007, 601, 5492-5498.	1.9	11
578	Palladium catalyzed mild reduction of α,β-unsaturated compounds by triethylsilane. Journal of Organometallic Chemistry, 2007, 692, 5113-5116.	1.8	26
579	Synthesis and photoluminescence properties of silicon nanowires treated by high-pressure water vapor annealing. Physica Status Solidi (A) Applications and Materials Science, 2007, 204, 1302-1306.	1.8	26
580	Porous silica-laser dye composite: physical and optical properties. Physica Status Solidi (A) Applications and Materials Science, 2007, 204, 1518-1522.	1.8	10
581	Wettability Switching Techniques on Superhydrophobic Surfaces. Nanoscale Research Letters, 2007, 2,	5.7	289
582	Infrared spectroscopy of self-assembled monolayer films on silicon. Surface Science, 2007, 601, 2566-2570.	1.9	4
583	Preparation and Characterization of Thin Films of SiOxon Gold Substrates for Surface Plasmon Resonance Studies. Langmuir, 2006, 22, 1660-1663.	3.5	68
584	Nanoscale Wettability of Self-Assembled Monolayers Investigated by Noncontact Atomic Force Microscopy. Langmuir, 2006, 22, 116-126.	3.5	51
585	Raman Imaging and Kelvin Probe Microscopy for the Examination of the Heterogeneity of Doping in Polycrystalline Boron-Doped Diamond Electrodes. Journal of Physical Chemistry B, 2006, 110, 23888-23897.	2.6	34
586	Localized electropolymerization on oxidized boron-doped diamond electrodes modified with pyrrolyl units. Physical Chemistry Chemical Physics, 2006, 8, 4924.	2.8	20
587	Well-Defined Carboxyl-Terminated Alkyl Monolayers Grafted onto Hâ^'Si(111):Â Packing Density from a Combined AFM and Quantitative IR Study. Langmuir, 2006, 22, 153-162.	3.5	172
588	Stability of the Gold/Silica Thin Film Interface:  Electrochemical and Surface Plasmon Resonance Studies. Langmuir, 2006, 22, 10716-10722.	3.5	52
589	Water Exclusion at the Nanometer Scale Provides Long-Term Passivation of Silicon (111) Grafted with Alkyl Monolayers. Journal of Physical Chemistry B, 2006, 110, 5576-5585.	2.6	54
590	In situmonitoring of protein adsorption on functionalized porous Si surfaces. Journal of Vacuum Science and Technology A: Vacuum, Surfaces and Films, 2006, 24, 747-751.	2.1	14
591	Electrochemical investigation of gold/silica thin film interfaces for electrochemical surface plasmon resonance studies. Electrochemistry Communications, 2006, 8, 439-444.	4.7	50
592	Direct amination of hydrogen-terminated boron doped diamond surfaces. Electrochemistry Communications, 2006, 8, 1185-1190.	4.7	57
593	Organic monolayers as resist layers for Cu deposition on Si (111) surfaces. Journal of Electroceramics, 2006, 16, 71-77.	2.0	2
594	Controlled growth of silicon nanowires on silicon surfaces. Journal of Electroceramics, 2006, 16, 15-21.	2.0	26

#	Article	IF	CITATIONS
595	A mild and efficient palladium–triethylsilane system for reduction of olefins and carbon–carbon double bond isomerization. Applied Organometallic Chemistry, 2006, 20, 214-219.	3.5	31
596	Bulk micromachining of silicon using electron-beam-induced carbonaceous nanomasking. Nanotechnology, 2006, 17, 5363-5366.	2.6	9
597	Synthesis and Optical Properties of Silicon Oxide Nanowires. Materials Research Society Symposia Proceedings, 2006, 958, 1.	0.1	0
598	Organic monolayers detected by single reflection attenuated total reflection infrared spectroscopy. Journal of Vacuum Science and Technology A: Vacuum, Surfaces and Films, 2006, 24, 668-672.	2.1	7
599	Thermal and photochemical isomerization of exocyclic 1,3-dienes: 1,1-diphenyl-3,4-bis(trimethylsilylmethylene)-1-silacyclopentane s-cis(E,E). Journal of Organometallic Chemistry, 2005, 690, 1028-1032.	1.8	2
600	Palladium-catalyzed protection of alcohols and cleavage of triethylsilyl ethers. Journal of Organometallic Chemistry, 2005, 690, 2372-2375.	1.8	26
601	Photochemical oxidation of hydrogenated boron-doped diamond surfaces. Electrochemistry Communications, 2005, 7, 937-940.	4.7	86
602	Palladium-Catalyzed Protection of Alcohols and Cleavage of Triethylsilyl Ethers ChemInform, 2005, 36, no.	0.0	0
603	Stable electroluminescence from passivated nano-crystalline porous silicon using undecylenic acid. Physica Status Solidi C: Current Topics in Solid State Physics, 2005, 2, 3273-3277.	0.8	14
604	Photoluminescence quenching of colloidal silver nanoparticle on porous silicon. , 2005, , .		0
605	Enhanced conductance of chlorine-terminated Si(111) surfaces: Formation of a two-dimensional hole gas via chemical modification. Physical Review B, 2005, 71, .	3.2	23
606	Colloidal Silver Nanoparticle Induced Photoluminescence Quench on the Surface Functionalized Planar Si. Materials Research Society Symposia Proceedings, 2005, 901, 1.	0.1	0
607	Protein Adsorption on the Surface Functionalized Planar Si. Materials Research Society Symposia Proceedings, 2005, 901, 1.	0.1	0
608	Chemical reactivity of hydrogen-terminated crystalline silicon surfaces. Current Opinion in Solid State and Materials Science, 2005, 9, 66-72.	11.5	133
609	Electron beam-induced modification of organic monolayers on Si(111) surfaces used for selective electrodeposition. Electrochemistry Communications, 2004, 6, 153-157.	4.7	29
610	Near edge X-ray absorption fine structure spectroscopy of chemically modified porous silicon. Journal of Electron Spectroscopy and Related Phenomena, 2004, 135, 143-147.	1.7	25
611	Bovine serum albumin adsorption on passivated porous silicon layers. Canadian Journal of Chemistry, 2004, 82, 1545-1553.	1.1	25
612	Hidden Electrochemistry in the Thermal Grafting of Silicon Surfaces from Grignard Reagents. Langmuir, 2004, 20, 6359-6364.	3.5	41

#	Article	IF	CITATIONS
613	Formation, Characterization, and Chemistry of Undecanoic Acid-Terminated Silicon Surfaces:Â Patterning and Immobilization of DNA. Langmuir, 2004, 20, 11713-11720.	3.5	171
614	Bovine serum albumin adsorption on functionalized porous silicon surfaces. , 2004, 5578, 99.		2
615	Palladium-Catalyzed Reduction of Olefins with Triethylsilane ChemInform, 2003, 34, no.	0.0	0
616	Palladium-catalyzed reduction of olefins with triethylsilane. Tetrahedron Letters, 2003, 44, 4579-4580.	1.4	36
617	A novel and efficient method for double bond isomerization. Journal of Organometallic Chemistry, 2003, 678, 1-4.	1.8	34
618	Effect of ruthenium cluster on the photoluminescence of chemically derivatized porous silicon. Applied Surface Science, 2003, 217, 125-133.	6.1	5
619	Nanopatterning of Si(111) surfaces by atomic force microscope scratching of an organic monolayer. Electrochemistry Communications, 2003, 5, 337-340.	4.7	19
620	Photoluminescence quenching of chemically functionalized porous silicon by a ruthenium cluster. Physica Status Solidi A, 2003, 197, 476-481.	1.7	2
621	Stabilization of porous silicon electroluminescence by surface passivation with controlled covalent bonds. Applied Physics Letters, 2003, 83, 2342-2344.	3.3	89
622	Microwave-Assisted Chemical Functionalization of Hydrogen-Terminated Porous Silicon Surfaces. Journal of Physical Chemistry B, 2003, 107, 13459-13462.	2.6	125
623	Effects of natural and electrochemical oxidation processes on acoustic waves in porous silicon films. Journal of Applied Physics, 2003, 94, 1243-1247.	2.5	16
624	A Brillouin scattering study of the effect of chemical passivation on the elastic properties of porous silicon. Semiconductor Science and Technology, 2002, 17, 692-695.	2.0	9
625	Thermal Hydrosilylation of Undecylenic Acid with Porous Silicon. Journal of the Electrochemical Society, 2002, 149, H59.	2.9	177
626	Structure Characterization of Porous Silicon Layers Based on a Theoretical Analysis. Langmuir, 2002, 18, 4165-4170.	3.5	5
627	Modification of Porous Silicon Surfaces with Activated Ester Monolayers. Langmuir, 2002, 18, 6081-6087.	3.5	65
628	Photoluminescence stabilization of anodically-oxidized porous silicon layers by chemical functionalization. Applied Physics Letters, 2002, 81, 601-603.	3.3	61
629	Brillouin spectroscopy of acoustic modes in porous silicon films. Physical Review B, 2002, 65, .	3.2	31
630	Determination of coverage in passivated porous silicon by Brillouin spectroscopy. Applied Physics Letters, 2001, 79, 4521-4523.	3.3	8

#	Article	IF	CITATIONS
631	Stability Enhancement of Partially-Oxidized Porous Silicon Nanostructures Modified with Ethyl Undecylenate. Nano Letters, 2001, 1, 713-717.	9.1	73
632	Ideal Passivation of Luminescent Porous Silicon by Thermal, Noncatalytic Reaction with Alkenes and Aldehydesâ€. Chemistry of Materials, 2001, 13, 2002-2011.	6.7	139
633	Second harmonic generation spectroscopy of chemically modified Si(111) surfaces. Surface Science, 2001, 488, 367-378.	1.9	23
634	"Reagentless―Micropatterning of Organics on Silicon Surfaces: Control of Hydrophobic/Hydrophilic Domains1. Journal of the American Chemical Society, 2001, 123, 1535-1536.	13.7	63
635	Pickled luminescent silicon nanostructures. Solid State Communications, 2001, 118, 319-323.	1.9	14
636	Passivated Luminescent Porous Silicon. Journal of the Electrochemical Society, 2001, 148, H91.	2.9	37
637	Chemical and thermal stability of titanium disilicide contacts on silicon. Journal of Applied Physics, 2001, 90, 1655-1659.	2.5	6
638	Thermal Functionalization of Hydrogen-Terminated Porous Silicon Surfaces with Terminal Alkenes and Aldehydes. Materials Research Society Symposia Proceedings, 2000, 638, 1.	0.1	3
639	Thermal Route for Chemical Modification and Photoluminescence Stabilization of Porous Silicon. Physica Status Solidi A, 2000, 182, 117-121.	1.7	88
640	Unprecedented effects of the trimethylsilyl group on the reactivity of 3C-silylated silacyclopentenes and their derivatives. Journal of Organometallic Chemistry, 2000, 604, 141-149.	1.8	4
641	Facile interfacial electron transfer through n-alkyl monolayers formed on silicon (111) surfaces. Electrochemistry Communications, 2000, 2, 562-566.	4.7	40
642	The preparation of flat H–Si(111) surfaces in 40% NH4F revisited. Electrochimica Acta, 2000, 45, 4591-4598.	5.2	157
643	Insights into the Formation Mechanisms of Siâ^'OR Monolayers from the Thermal Reactions of Alcohols and Aldehydes with Si(111)â^'H1. Langmuir, 2000, 16, 7429-7434.	3.5	199
644	Second Harmonic Generation at Chemically Modified Si(111) Surfacesâ€. Journal of Physical Chemistry B, 2000, 104, 7668-7676.	2.6	32
645	Les Sels de Bismuth (III) Comme Catalyseurs Dans la Reaction D'ouverture Des Epoxydes en Sere Siliciee. Phosphorus, Sulfur and Silicon and the Related Elements, 2000, 167, 81-92.	1.6	7
646	Controlled Functionalization and Multistep Chemical Manipulation of Covalently Modified Si(111) Surfaces1. Journal of the American Chemical Society, 1999, 121, 11513-11515.	13.7	212
647	Substituent Effects on the Reactivity of the Siliconâ~'Carbon Double Bond. Substituted 1,1-Dimethylsilenes from Far-UV Laser Flash Photolysis of α-Silylketenes and (Trimethylsilyl)diazomethane. Journal of the American Chemical Society, 1999, 121, 4744-4753.	13.7	33
648	New Synthetic Routes to Alkyl Monolayers on the Si(111) Surface1. Langmuir, 1999, 15, 3831-3835.	3.5	315

#	Article	IF	CITATIONS
649	Steady state and time-resolved spectroscopic studies of the photochemistry of 1-arylsilacyclobutanes and the chemistry of 1-arylsilenes. Canadian Journal of Chemistry, 1999, 77, 1136-1147.	1.1	9
650	The versatile behavior of the PdCl2/Et3SiH system. Conversion of alcohols to the corresponding halides and alkanes. Journal of Organometallic Chemistry, 1998, 554, 135-137.	1.8	41
651	Stereoselective synthesis of new hetero(P, Si, Ge, Sn)cyclic derivatives from zirconium diyne and diene complexes. Journal of Organometallic Chemistry, 1998, 564, 61-70.	1.8	12
652	Substituent Effects on the Reactivity of the Siliconâ^'Carbon Double Bond. Resonance, Inductive, and Steric Effects of Substituents at Silicon on the Reactivity of Simple 1-Methylsilenes. Journal of the American Chemical Society, 1998, 120, 9504-9512.	13.7	48
653	Far-UV laser flash photolysis in solution. A study of the chemistry of 1,1-dimethylsilene in hydrocarbon solvents. Journal of Photochemistry and Photobiology A: Chemistry, 1997, 110, 243-246.	3.9	17
654	PdCl2-Catalyzed Reduction of Organic Halides by Triethylsilane. Organometallics, 1996, 15, 1508-1510.	2.3	132
655	Zirconocyclisation: Access to new racemic (di) phosphines. Tetrahedron Letters, 1996, 37, 3109-3112.	1.4	21
656	SILA- AND GERMACYCLOPENTENES IN FUNDAMENTAL AND APPLIED ORGANOMETALLIC CHEMISTRY. Main Group Metal Chemistry, 1996, 19, .	1.6	14
657	Synthesis and characterization of poly(1-sila-cis-pent-3-enes) substituted with pendant pyridinyl groups. Journal of Inorganic and Organometallic Polymers, 1995, 5, 61-74.	1.5	4
658	5,10-dihydro-silanthrene as a reagent for the Barton-McCombie reaction. Tetrahedron Letters, 1995, 36, 3897-3900.	1.4	36
659	A MODIFIED McCORMACK SYNTHESIS OF 3-SILYLATED PHOSPHOL-3-ENES. Phosphorus, Sulfur and Silicon and the Related Elements, 1995, 105, 101-108.	1.6	4
660	PALLADIUM CHLORIDE-CATALYZED SYNTHESIS OF 1-X-1-ALKYL (OR 1-ARYL)-1-SILACYCLOPENT-3-ENES ( $X = Cl$ ,)	Tj <u>F</u> TQq0 (	D Q rgBT /Ove
661	1Η NMR SPECTRA OF 3-GERMABICYCLO[3.1.0]HEXANES AND 6-OXA-3-GERMABICYCLO[3.1.0]HEXANES. Main Group Metal Chemistry, 1995, 18, .	1.6	4
662	STUDY OF THE REGIOSELECTIVITY OF THE TRICHLOROSILYLATION OF ALLYLIC HALIDES. NOVEL 3-SILYL AND 3-GERMYL-1-SILA-3-CYCLOPENTENES. Main Group Metal Chemistry, 1994, 17, .	1.6	4
663	3,4-Functionalized silacyclopentanes. Synthesis of trans-4-amino-, azido- and alkyloxy-1-silacyclopentan-3-ols from 6-oxa-3-silabicyclo[3.1.0]hexanes. Journal of Organometallic Chemistry, 1994, 484, 119-127.	1.8	12
664	Spiro[3-germabicyclo[3.1.0]hexane-3,9'-[9]germafluorene]. Acta Crystallographica Section C: Crystal Structure Communications, 1994, 50, 1337-1339.	0.4	3
665	Synthèses de 3-silyl et de 3-germyl 1-sila et 1-germacyclopent-3-ènes. Journal of Organometallic Chemistry, 1993, 460, 155-161.	1.8	9
666	Regioselectivity in the trichlorosilylation of allylic halides. Synthesis of 1,1-dichloro-3-(methyldichlorosilyl)-1-silacyclopent-3-ene. Journal of Organometallic Chemistry, 1993, 444, 37-40.	1.8	13

#	Article	IF	CITATIONS
667	NMR Spectra of Organogermanium Compounds. Part XII.73Ge and13C NMR Spectra and Molecular Mechanics Calculations of 3-Germabicyclo[3.1.0]hexanes and Related Compounds. Bulletin of the Chemical Society of Japan, 1993, 66, 1732-1737.	3.2	5
668	Properties of Pt-Assisted Electroless Etched Silicon in HF/Na <sub>2</sub> S <sub>2</sub> O <sub>8</sub> Solution. Materials Science Forum, 0, 609, 231-237.	0.3	0
669	Chapter 7. Electrochemistry of graphene: The current state of the art. SPR Electrochemistry, 0, , 211-242.	0.7	4
670	Fullerene―C 60 / NH 2 : A recyclable heterogeneous catalyst for the green synthesis of chromene and pyrimidine derivatives and antibacterial evaluation. Journal of Heterocyclic Chemistry, 0, , .	2.6	2